Oikos
January 2010, Volume 119, Issue 1, Pages 10 - 26
http://dx.doi.org/10.1111/j.1600-0706.2009.17746.x

Multiple growth-correlated life history traits estimated simultaneously in individuals

Fabian Mollet[1,2,*], Bruno Ernande[3,2], Thomas Brunel[1,3], Adriaan D. Rijnsdorp[1,4]

[1] Wageningen IMARES, Inst. for Marine Resources and Ecological Studies, PO Box 68, NL-1970 AB IJmuiden, the Netherlands
[2] Evolution and Ecology Program, International Institute for Applied System Analysis IIASA, Schlossplatz 1, A-2361 Laxenburg, Austria
[3] IFREMER, Laboratoire Ressources Halieutiques, Avenue du Général de Gaulle, BP32, F-14520 Port-en-Bessin, France.
[4] Aquaculture and Fisheries group, Wageningen University, P.O.Box 338, NL-6700 AH Wageningen, The Netherlands

*: Corresponding author : F. Mollet, email address : Fabian.Mollet@wur.nl

Abstract:

We present a new methodology to estimate rates of energy acquisition, maintenance, reproductive investment and the onset of maturation (four-trait estimation) by fitting an energy allocation model to individual growth trajectories. The accuracy and precision of the method is evaluated on simulated growth trajectories. In the deterministic case, all life history parameters are well estimated with negligible bias over realistic parameter ranges. Adding environmental variability reduces precision, causes the maintenance and reproductive investment to be confounded with a negative error correlation, and tends, if strong, to result in an underestimation of the energy acquisition and maintenance and an overestimation of the age and size at the onset of maturation. Assuming a priori incorrect allometric scaling exponents also leads to a general but fairly predictable bias. To avoid confounding in applications we propose to assume a constant maintenance (three-trait estimation), which can be obtained by fitting reproductive investment simultaneously to size at age on population data. The results become qualitatively more robust but the improvement of the estimate of the onset of maturation is not significant. When applied to growth curves back-calculated from otoliths of female North Sea plaice Pleuronectes platessa, the four-trait and three-trait estimation produced estimates for the onset of maturation very similar to those obtained by direct observation. The correlations between life-history traits match expectations. We discuss the potential of the methodology in studies of the ecology and evolution of life history parameters in wild populations.

INTRODUCTION

The schedule according to which energy is allocated to either somatic growth or reproduction is a cornerstone of life history theory (Kooijman 1986, Roff 1992, Stearns 1992, Kozlowski 1996, Charnov, et al. 2001). Energy allocation schedules differ among species as they reflect adaptation to both the environment and internal constraints resulting from sharing a common currency between different functions. Individuals indeed face an energy trade-off between somatic growth and reproduction (Roff 1992, Stearns 1992, Heino and Kaitala 1999). In case of indeterminate growth, individuals also experience a trade-off between current and future reproduction since fecundity generally increases with body size. Various energy allocation schedules have been proposed in the literature (Von Bertalanffy and Pirozynski 1952, Day and Taylor 1997, Kooijman 2000, West, et al. 2001). They differ mostly in terms of priorities of energy flows to the different functions. Allocation schedules typically comprise four traits, namely energy acquisition, maintenance, onset of maturation, and thereafter reproductive investment, whereas somatic growth arises as a by-product: the energy that remains after accounting for the primary energy flows to maintenance and reproductive investment is available for somatic growth. The study of energy allocation schedules in individual organisms is difficult because of a lack of data at the individual level as this would require monitoring separate individual organisms throughout their life time. Studies therefore have focused on the population level as well as on single traits (Stevenson and Woods Jr. 2006). Studying the four traits together (acquisition, maintenance, onset of maturation and

reproductive investment) at the individual level would offer several advantages over the widely used single trait estimation at the population level: (1) phenotypic correlations between traits could be estimated; (2) changes in one trait could be interpreted conditionally on changes in other traits, precisely because of the previous correlations; (3) it would be more consistent with the fact that physiological trade-offs apply at the individual and not at the population level.

Organisms in which the individual growth history is recorded in hard structures offer a unique opportunity to study energy allocation schedules at the individual level. Fish for instance show indeterminate growth and the growth history of individuals can be reconstructed from the width of the seasonal structures imprinted in hard structures such as otoliths or scales (Runnström 1936, Rijnsdorp, et al. 1990, Francis and Horn 1997). Earlier studies have attempted to estimate the onset of maturation using growth history reconstructed from otoliths or scales (Rijnsdorp and Storbeck 1995, Engelhard, et al. 2003, Baulier and Heino 2008), but no study has yet attempted to simultaneously estimate several life history traits related to life time patterns of energy allocation at the individual level.

In this study, we estimate simultaneously parameter values at the individual level for energy acquisition, maintenance, onset of reproduction, and reproductive investment by fitting an energy allocation model to individual growth trajectories. The energy allocation model assumes that the onset of maturation is reflected in a discontinuity in the slope of the growth trajectory, while the energy acquisition discounted by maintenance is assessed by the slope of the growth trajectory before maturation, and reproductive investment is translated in the amplitude of the change in the slope of growth trajectory at the

discontinuity. The performance of the method and its sensitivity to both model uncertainty and inter-annual environmental variability are explored using simulated data. The method is applied to an empirical data set of individual growth curves back-calculated from otoliths of female North Sea plaice (*Pleuronectes platessa*). Maturity status deduced from the age and size at the onset of maturation estimated by our model is compared to direct evaluation of maturity status by visual inspection of the gonads in market sampling (Grift, et al. 2003).

MATERIAL AND METHODS

PARAMETER ESTIMATION

Energy allocation model. When an animal becomes mature, a proportion of the available energy is channeled towards reproduction and is no longer available for somatic growth (Ware 1982). Hence, a decrease in growth rate can be expected after maturation. We use a general energy allocation model (Von Bertalanffy and Pirozynski 1952, Charnov, et al. 2001, West, et al. 2001, Banavar, et al. 2002) according to which the growth rate of juveniles and adults is given by

$$\frac{\partial w}{\partial t} = \begin{cases} aw^{\alpha} - bw^{\beta} & \text{if} \quad t < t_{\text{mat}} \\ \\ aw^{\alpha} - bw^{\beta} - cw^{\gamma} & \text{if} \quad t \geq t_{\text{mat}} \end{cases} \tag{1}$$

where w is body weight, t is time, t_{mat} is time at the onset of maturation, aw^{α} is the rate of energy acquisition, bw^{β} is the rate with which energy is spent for maintenance and cw^{γ} is the rate of reproductive investment with which energy is spent for reproductive activity (e.g. gamete production, reproductive behavior). For simplicity we will refer to energy acquisition a, maintenance b and reproductive investment c, although a, b and c describe the size-specific rates for the corresponding processes. There is disagreement about the scaling exponents α, β, and γ involved in the allometries between energy rates and body weight. Metabolic theory of ecology (MTE) suggests that metabolism

scales with a quarter power law of body weight (West, et al. 1999, Gillooly, et al. 2001, Savage, et al. 2004). This hypothesis builds on the fractal-like branching pattern of distribution networks involved in energy transport (West, et al. 1997) but the generality of this allometric scaling law is contested (Banavar, et al. 2002, Darveau, et al. 2002, Clarke 2004, Kozlowski and Konarzewski 2004). Nevertheless, we assumed a scaling exponent of energy acquisition α=3/4 (West, et al. 1997) as this is close to empirical estimates of α (Gillooly, et al. 2001, Brown, et al. 2004) including our model species North Sea plaice (Fonds, et al. 1992). For the scaling exponent of maintenance β, it is required that $\beta > \alpha$ in order to obtain (i) bounded asymptotic growth, i.e. to reach an asymptotic maximum body weight in the absence of maturation and (ii) an energetic reproductive-somatic index (RSI), defined as the ratio of reproductive investment over body weight in terms of energy (in other terms an energetic analogue to the gonado-somatic index), that increases with age and size as commonly observed in empirical data (not shown). MTE suggests β=1 since with increasing size, the energy demand becomes relatively more important than its supply (West, et al. 1997, West, et al. 2001) and thus fulfills the required conditions. For the scaling exponent of reproductive investment γ, we assume $\gamma = 1$ for the sake of simplicity. This is in line with the assumption that total brood mass is a constant fraction of maternal body weight (Blueweiss, et al. 1978, Charnov, et al. 2001), although reproductive investment might be related to a body weight allometry with an exponent higher than 1 (Roff 1991).

By integration of Eq. (1) assuming $\alpha = 3/4$ and $\beta = \gamma = 1$, the somatic weight w can be expressed as a function of time t. To switch from juvenile ($t < t_{\mathrm{mat}}$) to adult ($t \geq t_{\mathrm{mat}}$)

growth in Eq. (1), a continuous logistic switch function $S(t)$ with an inflection point located at the time of the onset of maturation t_{mat} is used (Appendix A1). It results that the lifespan somatic growth curve is obtained as a continuous function of time though a discontinuity in its parameters due to the onset of maturation being introduced by the switch function $S(t)$:

$$w^{1-\alpha}(t) = (1 - S(t))\left[\frac{a}{b} - \left(\frac{a}{b} - w_0^{1-\alpha}\right)\mathrm{e}^{-b(1-\alpha)t}\right] + S(t)\left[\frac{a}{b+c} - \left(\frac{a}{b+c} - w_{\mathrm{mat}}^{1-\alpha}\right)\mathrm{e}^{-(b+c)(1-\alpha)(t-t_{\mathrm{mat}})}\right]$$

(3.0)

where w_0 is body weight at $t = 0$ and w_{mat} is body weight at $t = t_{\mathrm{mat}}$ given by

$$w_{\mathrm{mat}}^{1-\alpha} = \frac{a}{b} - \left(\frac{a}{b} - w_0^{1-\alpha}\right)\mathrm{e}^{-b(1-\alpha)t_{\mathrm{mat}}}. \tag{3.1}$$

The growth curve levels off at the asymptotic weight w_∞,

$$w_\infty^{1-\alpha} = a/(b+c). \tag{3.2}$$

Total reproductive investment R (including gonadic and behavioral costs) is obtained by integrating the rate of energy conversion to reproduction from t to $t + \Delta t$:

$$R(t + \Delta t) = \int_t^{t+\Delta t} c w(\tau)\,\mathrm{d}\tau, \tag{4}$$

where Δt describes the reproductive cycle over which the reproductive products are built up, fertilized and cared until the offspring is autonomous. An analytical expression of $R(t + \Delta t)$ as a function of $w(t)$ and $w(t + \Delta t)$ can be obtained (Appendix A2). Reproduction generally occurs at certain periods during lifespan. Fish for instance are

often annual spawners (including North Sea plaice) and hence reproductive investment is given over annual time steps ($\Delta t = 1$). Energy for reproduction is first stored in various body tissues during the feeding period and then re-allocated to the gonad and released during the spawning period. Since the currency of the model is energy, different energy densities of different tissues have to be accounted for when fitting the model to real data.

Fitting procedure. The energy allocation model was fitted using a general-purpose optimization procedure (R 2.6., optim) by restricting all parameters to be positive using box-constraints specification (Byrd, et al. 1995). Life history parameters a, b, c and t_{mat} were estimated by using this procedure to minimize the sum of squared residuals of weight at age data versus predicted weight at age. Q-Q-plots indicated that the distribution of residuals is close to normal. The algorithm was given a grid of possible combinations of a, b, c and t_{mat} as starting values and the best solution was selected based on the lowest AIC. A genetic algorithm (http://www.burns-stat.com/) yielded similar results as those presented in this paper (not shown). The estimates of the time at the onset of maturation t_{mat} and the asymptotic weight $w_{\infty}^{1/4} = a/(b+c)$ were constrained to a species-specific range (e.g. North Sea plaice 0.5yr$\leq t_{\mathrm{mat}} \leq$8.5yr, 400g$\leq w_{\mathrm{mat}} \leq$4000g).

Confounding. Preliminary analyses of the plaice data set (see below) has shown that the estimation of the 4 life history parameters a, b, c and t_{mat} (four-trait-estimation) yields an unimodal distribution for energy acquisition a but a bimodal distribution for maintenance b and reproductive investment c (Figure 1). The mode in the distribution of b is likely an underestimation at 0, which is related to an overestimation of c reflected in the 2nd mode of its distribution. Selection of observations belonging to the 2nd

mode of the b distribution thanks to a Gaussian mixture model (R 2.6., MClust, Fraley and Raftery 2006) also removes the 2nd mode in the c distribution (dotted line, Figure 1). To remove the confounding between b and c several options were considered: 1) use only observations belonging to the 2nd b-mode – the correlation structure in these observations was considered to be the most representative (Table 3) and was used for simulations – or 2) assume parameter b to be fixed at the population level (three-trait estimation). The rationale for this choice is that maintenance costs are generally acknowledged to be species- rather than individual-specific (Kooijman 2000) and our main interest is in variation in reproductive investment. The population level value of b was estimated by fitting a mean growth trajectory (Eq. 1) to the whole somatic weight-at-age dataset. Confounding between b and c on this level was avoided by fitting concomitantly reproductive investment $R(t+\Delta t)$ to an independent dataset of reproductive investment-at-age (see application to real data). The partitioning of b in the sum $b+c$ could thereby be estimated accurately. The population mean growth trajectory and reproductive investment were fitted simultaneously by minimizing the sum of weighted squared residuals of somatic weight-at-age data and reproductive investment-at-age data versus their predictions.

PERFORMANCE ANALYSIS

Performance. To test its performance, the method was applied to 2000 growth trajectories simulated with known life history parameters. The life history parameters a, b, c and t_{mat} were drawn from a multivariate normal distribution with the co-variance matrix taken from the results of the application to North Sea plaice data, after having selected only observations belonging to the representative b-mode in the distribution of

parameter estimates (see above, Table 3). To simulate weight-at-age data, $w(t+\Delta t)$ was expressed as a function of $w(t)$ by using a function similar to Eq. (3) but in which $w^{1-\alpha}(t)$ was replaced with $w^{1-\alpha}(t+\Delta t)$, and $w_0^{1-\alpha}$ (for $t \le t_{\text{mat}}$) and $w_{\text{mat}}^{1-\alpha}$ (for $t > t_{\text{mat}}$) with $w^{1-\alpha}(t)$. To evaluate the estimation bias on the population level and assess its dependency on life-history strategy and environmental variability, the mean relative bias over all life history parameters (the average absolute difference between estimated and true values relative to true values) was used for each individual i as a measure of accuracy:

$$e_i = \frac{1}{4}\left(\frac{\left|a_{\text{est}} - a_{\text{true}}\right|}{a_{\text{true}}} + \frac{\left|b_{\text{est}} - b_{\text{true}}\right|}{b_{\text{true}}} + \frac{\left|c_{\text{est}} - c_{\text{true}}\right|}{c_{\text{true}}} + \frac{\left|t_{\text{mat,est}} - t_{\text{mat,true}}\right|}{t_{\text{mat,true}}} \right) \tag{5}$$

To test performance in the deterministic case, i.e. without environmental variability, the bias e_i was analyzed in dependence of a combination of two of the following factors: (i) the relative reproductive investment $q = c/(b+c)$, (ii) the relative onset of maturation $\tau = t_{\text{mat}}(b+c)$, (iii) the relative initial size $\nu_0 = w_0(a/(b+c))^{-4}$, (iv) age t and (v) the number of observations in the mature stage y_{mat}. Variation in the three dimensionless parameters q, τ and ν_0 accounts for any variation in the parameters they are comprised of, i.e. a, b, c, t_{mat} and w_0, which allows investigating the whole parameter space at a smaller cost.

Effects of temporal variability in environmental conditions. Individual growth trajectories will be affected by environmental variability. To test whether the parameters corresponding to energy acquisition a, maintenance b, reproductive investment c and

time at the onset of maturation t_{mat} can be estimated reliably, annual stochasticity was introduced in the individuals' life-history traits drawn from the multivariate normal distribution (see deterministic case). As environmental variability is likely to be auto-correlated, for simplicity a first order autoregressive process AR(1) was used to simulate the lifespan series of the energy acquisition parameter a (constrained to be positive):

$$a_t = E(a) + \theta(a_{t-1} - E(a)) + \varepsilon_t \qquad \varepsilon_t \sim N(0, \sigma_a^2(1-\theta^2)) \qquad (6)$$

where $E(a)$ denotes the expected value of a, θ is the autoregressive parameter and ε_t is a normally distributed noise term with mean 0 and variance $\sigma_a^2(1-\theta^2)$ where σ_a^2 is the variance of a_t. The corresponding series of b_t and c_t were simulated by sampling b_t and c_t from the normal distributions that yielded correlations with the autoregressive a_t series which were the same as those observed among the individual estimations. The rationale here is that we assume that observed correlations between energy acquisition and other life history traits across individuals are mainly due to plastic physiological processes (versus genetic correlations) that therefore can also apply within individuals through time in case of temporal variation in energy acquisition. More precisely, b_t and c_t were sampled from the normal distributions $N(\beta_0 + \beta_1 a_t, \sigma)$ that yielded linear regressions of parameters b and c on a that were consistent with observed means, variances and correlations, that is with intercept β_0, slope β_1 and residual variance σ^2 defined as:

$$\beta_0 = \bar{x} - \bar{a}\beta_1 \qquad \beta_1 = \frac{\rho(a,x)\sigma_x}{\sigma_a} \qquad \sigma^2 = \sigma_x^2 - \beta_1^2\sigma_a^2 \qquad (7)$$

where x stands for b or c and the means $\bar{x}$ and $\bar{a}$, variances σ_x^2 and σ_a^2, and correlations $\rho(a,x)$ were taken from the empirical results of the application to North Sea plaice $r(a,x)$ (see Table 3). Body weight was constrained to be monotonously increasing while prioritizing reproduction over growth. Available surplus energy $aw^{3/4} - bw$ was first allocated to reproduction and the remaining energy thereafter $aw^{3/4} - (b+c)w$ was allocated to growth. If surplus energy happened to be negative $aw^{3/4} - bw < 0$ acquisition a and maintenance b were resampled until obtaining a positive amount. If the remaining energy was negative $aw^{3/4} - (b+c)w < 0$, reproductive investment c was adjusted such that all available surplus energy was used for reproduction and none for somatic growth by setting $c = aw^{-1/4} - b$. The initial conditions of the simulation were chosen such that the realized θ_a of the initial at-series was within [0,1], and that the realized CV's in a, b and c where within [0,0.5]. In addition to the relative reproductive investment q, timing of onset of maturation τ and initial weight ν_0, the effect of the expected value $E(x)$ of the parameters (x standing for a, b or c), the realized coefficients of variation of the parameters CV_x, the realized degree of auto-correlation θ_x, and the realized correlation $r_{\text{sim}}(x,x')$ between the simulated series of a, b and c, the age t and the number of observations in the mature stage y_{mat} on the mean of bias percentages (Eq. 5) was analyzed by a linear model:

$$e = \beta_0 + \beta_1 q + \beta_2 \tau + \beta_3 \nu_0 + \beta_4 t + \beta_5 y_{\text{mat}} + \beta_6 CV_x + \beta_7 \theta_x + \beta_8 r(x,x') + \varepsilon \qquad (8)$$

where the β's are the statistical parameters and ε is a normal error term (also in all subsequent statistical models). In this case the true values of parameters a, b and c used

for bias computation (see Eq. 5) were the geometric means of the respective realized time series

Model uncertainty. The effect of uncertainty about the scaling exponent α of energy acquisition rate with body weight was explored by fitting an energy allocation model to the generated deterministic data set (i.e. without environmental noise) postulating a scaling exponent lower (α = 2/3) or higher (α = 4/5) than the one used to generate the data (α = 3/4). A wrong assumption on α would lead to a different population level estimate of the fixed b and the effect of uncertainty about α in this approach was explored along the same line as above.

APPLICATION TO DATA

Data. The method developed was applied to an empirical dataset of individual growth trajectories back-calculated from otoliths of 1779 female North Sea plaice from cohorts from the 1920s to the 1990s, aged at least 6 years (Rijnsdorp and Van Leeuwen 1992, Rijnsdorp and Van Leeuwen 1996). This age threshold was chosen as these females then have 90% probability of being sexually mature for at least one year (Grift, et al. 2003). Because the otolith samples were length stratified, the observations of each length class were weighted according to its relative frequency in the population to obtain population level estimates.

Length-weight relationship. The back-calculated growth trajectories, which are in body length units (l in cm), were converted into body weight (w in g). We used the relationship between body weight w and length l of post spawning fish, estimated from market sampling data by a linear model. The rationale was that spent fish have a low condition, i.e. there are no energy reserves for reproduction in the post-spawning state:

$$\log(w) = \beta_0 + \beta_1 d^1 + \beta_2 d^2 + \beta_3 d^3 + \beta_3 \log(l) + \varepsilon \quad (9)$$

where d is the day in the year accounting for the high condition early in the year before spawning, the condition low after spawning and the building up of resources thereafter. The body weight at $w_0 = w(t = 0)$ was assumed to be constant across individuals and equal to 2.5mg corresponding to the weight of fish as large as the circumference of an egg with a radius of 2mm (Rijnsdorp 1991).

Maintenance. To avoid confounding between parameters, maintenance b was assumed to be fixed across individuals at its population level estimate (see section confounding above). To obtain this estimate, the population mean growth trajectory and an independent estimate of reproductive investment (see details below) were fitted simultaneously by minimizing the sum of weighted squared residuals of somatic weight-at-age data and reproductive investment-at-age data versus their predictions. The population level estimates assuming the scaling exponent α=3/4 were a=4.84.g$^{1/4}$.yr^{-1}, b=0.47 yr^{-1}, c=0.40 yr^{-1}, t_{mat}=4.00 yr (Figure 2). The population $b_{\alpha=3/4}$=0.47 yr^{-1} (see results) was used as a constant in the three-trait estimation.

Reproductive investment. Reproductive investment data included the cost of building gonads as well as the cost of migration between the feeding and spawning grounds. Reproductive investment R_{somatic}, expressed in units of energy-equivalent somatic weight, was thus obtained as

$$R_{\text{somatic}} = p_{\text{adult}}(g\kappa + M_{\text{resp}} / \delta) \quad (10)$$

where p_{adult} is the probability of being mature, g is the gonad weight, κ is the conversion factor to account for different energy densities between gonad and soma, M is the energy spent for migration and δ is the energy density of soma. Gonad weight g and the probability of being mature p_{adult} were estimated as functions of size or age and size, respectively, using linear models fitted to market samples of pre-spawning females:

$$\log(g) = \beta_0 + \beta_1 \log(l) + \varepsilon \tag{11}$$

Gonad weight was set to zero for females for which the probability of being mature p_{adult} was less than 50%, given age and size:

$$\text{logit}(p_{\text{adult}}) = \beta_0 + \beta_1 t + \beta_2 l + \beta_3 t \times l + \varepsilon \tag{12}$$

The factor used to convert gonad weight g to energy-equivalent somatic weight was κ=1.75, corresponding to the ratio between energy densities in pre-spawning gonad and in post-spawning soma (Dawson and Grimm 1980). Migration cost was estimated assuming a cruising speed V of 1 body length per second (Videler and Nolet 1990). The migration distance D is positively related to body size (Rijnsdorp and Pastoors 1995) with an average of about 140 nautical miles for a body length of 40cm in plaice (Bolle, et al. 2005). The energetic cost of swimming is then given by:

$$M_{\text{resp}} = (10^{0.3318} V (77.9T + 843.3) w^{3/4}) D / V \tag{13}$$

where M_{resp} is the respiration rate in J per month (Priede and Holliday 1980), D/V is the duration of active migration (in months) and T is temperature in °C, set to 10°C. The energy spent for respiration M_{resp} was converted into energy-equivalent somatic weight

assuming an energy density in post-spawning condition of δ=4.666kJ.g^{-1} (Dawson and Grimm 1980).

The resulting size-dependent energy-based reproductive investment relative to the somatic weight, i.e. the reproductive-somatic index RSI, increased with length l, and the resulting gonadic investment relative to the reproductive investment, i.e. the gonado-reproductive index GRI, was minimal for intermediate size classes (Figure 3). Using this model, an average plaice of 40cm length had a reproductive investment, expressed as a percentage of the post-spawning body weight, of about 38.0%, of which about 86% is used for gonads and 14% for migration.

Validation. To validate the approach, the estimates of the time at the onset of maturation t_{mat} were compared to independent estimates. Since t_{mat} is estimated in continuous time but reproduction occurs only at the start of the year, the age at first spawning A_{mat} was estimated by rounding up t_{mat} to the next integer, assuming a minimal time interval of 4 months between the onset of maturation and the actual spawning season ($A_{\mathrm{mat}} - t_{\mathrm{mat}} \geq 1/3$ year). These 4 months correspond to the minimal period of time during which gonads are built up in typical annual spawners (Rijnsdorp 1990, Oskarsson, et al. 2002). From the estimated A_{mat}, the probabilities of becoming mature at given ages and sizes were estimated and compared to estimates obtained from independent population samples (Grift, et al. 2003). Since the individuals' age at first spawning A_{mat} was known, the probability of becoming mature was estimated directly by logistic regression of the ratio between the number of first time spawners and the number of juveniles plus first time spawners (in population samples, first time and repeat spawners can usually not be

distinguished and the fraction of first spawners has to be estimated separately). As in Grift, et al. (2003), the probability of becoming mature was modeled as:

$$\text{logit}(p_{\text{mat}}) = \beta_0 + \beta_{YC} YC + \beta_t t + \beta_l l + \beta_{YCt} YC \times t + \beta_{YCl} YC \times l + \beta_{tl} t \times l + \varepsilon \qquad (14)$$

i.e., the probability of becoming mature p_{mat} depended on the individuals' year class YC (cohort), age t and length l. Year class was treated as a factor while age and length were treated as continuous variables. The probability of becoming mature p_{mat} is also referred to as the probabilistic maturation reaction norm (PMRN, Heino, et al. 2002) and is usually visualized using the 50% probability isoline in the age-length plane (also referred to as the PMRN midpoint or L_{P50}).

RESULTS

PERFORMANCE ANALYSIS

Parameter estimation in the deterministic case. When data are simulated deterministically, i.e. without environmental noise, the bias in the life history parameter estimation is negligible over the observed (estimated) range of values for both, the four-trait and the three-trait estimation (Figure 4). The errors in the b-estimate are positively correlated to errors in the estimates of a and t_{mat} and negatively correlated to errors in the estimate of c (Table 1), but this might not be very meaningful since the averages of biases are about 0. In the three-trait estimation, maintenance b was assumed to be constant to avoid confounding with reproductive investment c (see below). For the four-trait estimation, biases might arise if there are too few observations y_{mat} of the mature status, if the relative onset of maturation τ is early and if the relative reproductive investment q is small (Figure 4). The trends in the three-trait estimation are similar but relative biases are lower and the relative influence of q on the bias is much less important (Figure 4).

Parameter estimation in the stochastic case. The suspected confounding between maintenance b and reproductive investment c was confirmed by the results on simulated data with environmental variability: 1) Although the co-variance structure used to simulate data was taken from selected modes in the trait distribution estimated from real data, the trait estimates obtained from these simulated data resulted in multimodal distributions (Figure 5) very similar to those found in the estimates from real data (see

Figure 1 & 2). The estimation errors of b and c were negatively correlated ($r_e(b,c)$=-0.67, Table 1, Figure 5), whereas the bias in the sum of $b+c$ was much lower than in its separate compounds b and c (18% vs. -32 and 23% average deviation, Table 1, Figure 5). Hence, the sum $b+c$ is relatively well estimated but its partitioning between b and c is prone to error since an underestimation of maintenance b is compensated by an overestimation of reproductive investment c and *vice versa*. This correlation between estimation errors of b and c thus results in artifact modes in their trait distributions. If $b+c$ is overestimated, acquisition a has to be overestimated to fit a similar asymptotic weight, therefore the high positive correlation between biases in a and $b+c$ ($r_e(a,b+c)$=0.93, Table 1, Figure 5). Overestimation in t_{mat} might compensate for overestimation in a or $b+c$ in the same way (not shown). The confounding could not be removed by simply constraining the b-estimates above a certain positive threshold: the parameter distribution turned out to be bimodal too, with the first mode around the threshold instead of being around 0 (not shown). The unimodal distributions in the deterministic case (not shown) indicate that confounding mainly arises due to the interannual environmental stochasticity in the parameters along the growth trajectory.

Effects of environmental variability on parameter estimation. Environmental noise increases the overall bias (Eq. 5). For four-trait estimation, bias most dramatically increases with variation in the energy acquisition CV_a as shown by the regression against potentially explanatory variables (Eq. 8; Table 2). Furthermore, estimations are more reliable, if relative reproductive investment q, the number of observations (age t), and the correlation between a and b, $r(a,b)$ are high but also if relative onset of maturation

τ and the number of mature observations y_{mat} are low (Table 2). In the three-trait estimation, the signs of the effects of age t and relative onset of maturation τ are inversed, relative reproductive investment q and the number of reproductive events do not explain variation in bias but additional variation is explained by CV_c, the auto-correlations θ_a and θ_c and the correlation $r(a,c)$ instead of $r(a,b)$.

Figure 6 shows the bias in the estimates of the life history parameters against the average realized CV's. As expected, the variance and bias in the estimates typically increase with the overall CV (Figure 4) and the bias is on average higher in the four-trait estimation than in the three-trait estimation. Generally, the variability in parameters results in an underestimation of a and b and a slight overestimation in t_{mat} relative to their mean (Figure 6). Reproductive investment c is generally overestimated relative to its geometric mean in the four-trait estimation but slightly underestimated in the three-trait estimation. Recall that the bias is defined relative to the realized geometric mean of the parameter time series, and part of it may therefore not really represent estimation inaccuracy since no real true value can be defined in this case (what is estimated does not necessarily correspond to the geometric mean of the time series). Only the bias in t_{mat} is strictly defined here.

The age at onset of maturation t_{mat} or age at first maturity A_{mat} are generally overestimated for the early maturing individuals (Table 4). This overestimation is smaller in the three-trait estimation but on the other hand, many individuals are assigned to mature at the earliest possible age in this approach. A very early maturation might be the best solution in the energy allocation model fitting if no breakpoint can be detected in the

growth curve. The confounding of parameters a, b and c does not seem to influence the accuracy of t_{mat}-estimates significantly, since the similarity between confounded estimates of t_{mat} or A_{mat} and estimates where the confounding has been removed is very high (see below, Table 4).

Effect of model uncertainty on parameter estimation. Figure 7 shows the true against the estimated values of the life history parameters in the deterministic case when the scaling exponent α of energy acquisition rate with body weight was assumed to be lower (α = 2/3) or higher (α = 4/5) in the model fitted to the data than in the one used to simulate the data (α = ¾). For different scaling exponents, different population level estimates of the parameters are obtained so that the value of fixed maintenance in the three-trait estimation differs: $b_{\alpha=2/3}$=0.33 yr^{-1}, $b_{\alpha=3/4}$=0.47 yr^{-1}, $b_{\alpha=4/5}$=0.88 yr^{-1}. Asymptotic body weight $w_{\infty}^{1/4} = a/(b+c)$ is always estimated accurately (not shown). If α is assumed too low (α = 2/3), acquisition a and time at the onset of maturation t_{mat} are generally overestimated, whereas maintenance b and reproductive investment c are generally underestimated and *vice versa* if α is assumed too high (α = 4/5). The effect of an erroneous assumption on the fixed value of maintenance b in the three-trait estimation was also evaluated. It had a negligible effect, resulting in a very small and constant bias in parameters estimates for an assumption on b deviating by 10% from the true value (not shown).

APPLICATION to North Sea Plaice

The algorithm converged in 99% of the cases. The average estimates of life history parameters, after removing the estimations corresponding to the artifact mode in the

distribution of b estimates, were a=5.31 $g^{1/4}.yr^{-1}$, b=0.57 yr^{-1}, c =0.32 yr^{-1} and t_{mat}=4.45 yr (Table 3). Onset of maturation t_{mat} was negatively correlated with acquisition a, $r(a,t_{mat})$=-0.22, and reproductive investment c , $r(c,t_{mat})$=-0.63, but positively correlated with maintenance b, $r(b,t_{mat})$=0.30 (Table 3). The correlation between a and $b+c$ was highly positive, $r(a,b+c)$=0.93. When using the three-trait estimation procedure, i.e. assuming a maintenance fixed at its population level value b=0.47, the following average parameter estimates were obtained: a=5.29 $yr.g^{-1-\alpha}$, c=0.41 $yr.g^{-1}$, t_{mat}=3.53 yr (Table 3). In this case, the correlation between a and t_{mat}, $r(a,t_{mat})$ =–0.68, and between a and c , $r(a,c)$=0.91, were stronger. The correlation between a and c equals by definition the correlation between a and $b+c$ under the four-trait estimation (Table 3).

The four-trait and the three-trait estimation give roughly the same results for the timing of maturation t_{mat} or A_{mat} (Table 4). The similarity of the A_{mat} estimate between the two approaches increases slightly, when only the observations belonging to the 2nd b-mode are considered. The elimination of the confounding between maintenance b and reproductive investment c by estimating only three traits or by selecting the 2nd b-mode in the four-trait procedure does not affect the accuracy of the t_{mat} estimate.

The probabilistic maturation reaction norms or PMRNs were derived only for cohorts YC comprising at least 30 observations and showed a good match with those obtained by Grift, et al. (2003) averaged over the same cohorts (Figure 8). For the maturation-relevant ages, i.e. age 3 and 4, they are almost identical. The slope of the PMRN estimated here is lower than the one in Grift, et al. (2003).

DISCUSSION

Model assumptions. The method developed in this paper is the first to estimate simultaneously the different life history parameters related to the energy allocation schedule (energy acquisition, maintenance, onset of maturation and reproductive investment) from individual growth trajectories. We restricted ourselves to a Von Bertalanffy-like model, but, alternatively, structurally different energy allocation models, such as net production or net assimilation models (Day and Taylor 1997, Kooijman 2000), could be used. The performance analysis shows that the method with a Von Bertalanffy-like model can be expected to give accurate results as long as the scaling exponents of the allometric relationships between the underlying energy allocation processes (energy acquisition, maintenance, reproduction) and body weight applied in the estimation are correct. Even if they are not, the results are still expected to be qualitatively sound, and the resulting biases are predictable.

For the sake of simplicity, the scaling exponents of maintenance β and reproductive investment γ, here assumed to be 1, were neither estimated nor tested for their effects on estimation error, because a value different from 1 would require solving numerically the differential equations describing energy allocation at each iteration. Applying equal scaling exponents for energy acquisition and maintenance, i.e. $\alpha = \beta$, as suggested for instance by Day and Taylor (1997) and Lester, et al. (2004), resulted in unrealistic behavior of the energetic reproductive-somatic index RSI, suggesting that the scaling exponent of maintenance needs to be higher than the exponent of energy acquisition.

Based on theoretical (West, et al. 1997) and empirical case-specific evidence (Fonds, et al. 1992), as well as on realistic asymptotic weight and RSI, we conclude that applying scaling exponents following the inequalities $\alpha < \beta$ and $\alpha < \gamma$ are a good starting point for the estimation of individual life history parameters.

Performance analysis. For practical applications, the method should be applied to data on individuals for which two or more observations of the mature state are available. In this case the estimation error is negligible in a deterministic setting over the range of realistic (observed) parameter combinations. Environment variability in life history parameters leads to a slight underestimation of the average parameters for energy acquisition at and maintenance b_t and an overestimation of reproductive investment c_t (not in the three-trait estimation) but the onset of maturation t_{mat} is on average correctly estimated. With increasing environmental noise the average biases increase (except for the maintenance b) and estimation precision decreases (Figure 4). Variability in a_t has the largest impact on bias and the relative reproductive investment q might have to stay above a certain level to minimize the bias (Table 2). The negative effect on the bias of age is balanced by a positive effect of relative onset of maturation τ and of the number of adult observations y_{mat} and the interpretation of the deterministic case, where y_{mat} had a negative effect on the bias, therefore not necessarily falsified. However, these biases should be interpreted with caution because they were computed relative to the geometric mean of the simulated parameter time series, which does not correspond to a 'true' value as in the deterministic case. In other terms, there is no natural 'true' value to be compared with estimates in the stochastic case, except for t_{mat}.

Life-history correlation. (Co-)variation in (between) life history parameters at the phenotypic level, i.e. as observed across individuals, results from a genetic and an environmental (plastic) source of (co-)variation (Lynch and Walsh 1998). From life history theory (Roff 1992, Stearns 1992) we expect that 1i) juvenile growth rate $\partial w_{\text{juv}} / \partial t$ and age at maturation t_{mat} are negatively correlated $\rho(\partial w_{\text{juv}} / \partial t, t_{\text{mat}}) \leq 0$ - the higher the juvenile growth rate is, the earlier the individual will hit a presumably fixed genetically determined PMRN and mature – and 1ii) size-specific reproductive investment RSI and age at maturation t_{mat} are negatively correlated $\rho(\text{RSI}, t_{\text{mat}}) \leq 0$. From the assumptions of our bioenergetic model it is given that 2i) juvenile growth rate $\partial w_{\text{juv}} / \partial t$ increases with size-specific energy acquisition rate a, resulting in a positive correlation $\rho(\partial w_{\text{juv}} / \partial t, a) \geq 0$; 2ii) juvenile growth rate $\partial w_{\text{juv}} / \partial t$ decreases with size-specific maintenance rate b, resulting in a negative correlation $\rho(\partial w_{\text{juv}} / \partial t, b) \leq 0$; and 2iii) size-specific reproductive investment RSI increases with size-specific reproductive investment rate c, resulting in a positive correlation $\rho(\text{RSI}, c) \geq 0$. Life history theory and our model assumptions together thus lead to the following expectations: 3i) size-specific energy allocation rate a is negatively correlated with age at maturation t_{mat}, $\rho(a, t_{\text{mat}}) \leq 0$; 3ii) size-specific maintenance rate b is positively correlated with age at maturation t_{mat}, $\rho(b, t_{\text{mat}}) \geq 0$; and 3iii) size-specific reproductive investment rate c is negatively correlated with age at maturation t_{mat}, $\rho(c, t_{\text{mat}}) \leq 0$. The correlations between a, b and c cannot be easily interpreted in terms of life history theory but can be in the light of our model: since the asymptotic size $w_{\infty}^{1/4} = a/(b+c)$ is roughly constant within a species, increases in size-specific energy acquisition a or in speed of growth $(b+c)$

are reciprocally compensated to stabilize w_∞. The construction of the model therefore imposes $\rho(b,c) \leq 0$ and $\rho(a,b+c) \geq 0$, the only degrees of freedom being $\rho(a,c)$ and $\rho(a,b)$.

In terms of environmental variation, energy acquisition a might be externally influenced by variable food availability, maintenance b, interpreted here as the resting metabolic rate (i.e. the increase in maintenance due to higher consumption is accounted for by a), might be externally influenced by variability in temperature only and reproductive investment c might vary with the annually stored energy resources. From the environmental co-variation, the correlations $\rho(a,c)$ and $\rho(a,b)$ might be expected across individuals and within the lifespan of an individual: the positive effect of temperature on both food availability due to increased productivity of the system, and hence a, and metabolic rates, hence b, may lead to a positive correlation $\rho(a,b) \geq 0$; the energy resources available for reproductive investment (gonadic tissue, spawning migration) is determined by the energy which is physiologically made available and hence likely mainly by a, causing a positive correlation $\rho(a,c) \geq 0$ on the phenotypic level according to the rule "the more resources are available, the more can be spent".

The signs of the correlations between life history parameters obtained for plaice (Table 3) matched the previous theoretical expectations. Most importantly, we find $r(a,t_{\text{mat}}) \leq 0$, $r(b,t_{\text{mat}}) \geq 0$ and $r(c,t_{\text{mat}}) \leq 0$. These correlations also might be to some degree due to the correlation between estimation errors (Table 1) but not entirely, since the correlations between the traits are higher than between the errors (and the absolute traits are larger than the errors). The correlations $r(b,c)$ and $r(a,b+c)$ are indeed found to be due to the

correlations between estimation errors (Table 1) and thereby contribute, by construction of the model, to stabilize the asymptotic weight w_∞ (see above). The $r(a,b)$ might also be partly due to the error correlation. However, $r(a,c)$ is not, since the errors in a and c are negatively correlated, whereas the found $r(a,c)$ is about 0. This indicates that the true $r(a,c)$ might in fact be positive. In the three-trait estimation, $r(a,c)$ =0.91 is indeed highly positive, suggesting that the $r(a,c)$ found in the four-trait estimation might be due to the confounding with maintenance rate b. By assuming a constant b in the three-trait estimation, the co-variances between the three traits a, c and t_{mat} are inflated. The correlation $r(a,c)$ in the three-trait estimation becomes equal to the correlation $r(a,b+c)$ in the four-trait estimation, due to the classical relationship of covariances $\text{cov}(a,b+c) = \text{cov}(a,b) + \text{cov}(a,c)$. In the three-trait estimation $\text{cov}(a,c)$ is inflated by artificially fixing b and thereby forcing the covariance $\text{cov}(a,b) = 0$ to nullity so that $\text{cov}(a,b+c) = \text{cov}(a,c)$.

Application to real data. The method validation was based on the comparison between estimates of the timing of the onset of maturation t_{mat} obtained from back-calculated growth trajectories and independent estimates obtained from biological samples from the spawning population. Both estimation procedures are subject to error but similar patterns should nevertheless indicate the likelihood of both. For the ages at which maturation mainly occurs (around age 4), the PMRN based on our estimates is very similar to the PMRNs based on biological samples from the population (Grift, et al. 2003). The relatively higher and lower maturation probability for younger and older ages respectively is likely due to extrapolation to ages at which only few fish become mature

and the estimation becomes less reliable. If the interval between the start of energy allocation to reproduction t_{mat} and the subsequent age at first spawning A_{mat} was assumed to be less or more than 4 months, the resulting reaction norm would be lower or higher respectively in the age-size plane. However, for plaice 4 months correspond to the time interval between the onset of vitellogenesis (August, September) and the midpoint of the spawning season (Rijnsdorp 1990, Oskarsson, et al. 2002). The good correspondence between the two estimation methods of the PMRN suggests that environmental variability is unlikely to have been so high as to result in biases as high as in the simulation analysis (see biases of t_{mat} in Figure 4).

Reproductive investment. Reproductive investment was modeled including a size-dependent gonadic investment and a size-dependent cost of migration. The modeled energetic reproductive-somatic index RSI (energy-based reproductive investment relative to somatic weight) is increasing with somatic weight as is the modeled gonado-reproductive index GRI (gonadic relative to reproductive investment) and consequently the resulting gonado-somatic index GSI (gonadic weight relative to somatic weight). This is in line with the expectation since data show that GSI increases with size (Rijnsdorp 1991). In contrast, the modeled migration cost relative to reproductive investment (1-GSI) decreases with size. Since migration distance increases with fish size (Rijnsdorp and Pastoors 1995, Bolle, et al. 2005), the advantage of feeding offshore must be relatively more important than the migration cost.

Possible extensions. The method proposed here can be applied to a variety of organisms in which the annual pattern in somatic growth is reflected in hard structures: scales or otoliths in fish (Rijnsdorp, et al. 1990, Panfili and Tomas 2001, Colloca, et al. 2003),

shells in bivalves (Witbaard, et al. 1997, Witbaard, et al. 1999), endoskeleton in echinoderms (Pearse and Pearse 1975, Ebert 1986, Gage 1992), teeth in mammals (Laws 1952, Godfrey, et al. 2001, Smith 2004) or skeleton in amphibians (Misawa and Matsui 1999, Kumbar and Pancharatna 2001) and reptiles (Zug, et al. 2002, Snover and Hohn 2004). If a back-calculation method from the hard structures can be validated, the analysis of individual growth trajectories with the method developed in this paper offers the opportunity to study a variety of life history trade-offs without the need to follow individuals throughout their lifetime using experiments in controlled conditions or methods such as mark-recapture. The method holds for any other frequency of age and size observations and for any other frequency of spawning than the here illustrated annual observations and annual spawning intervals. Under the assumption that energy is allocated to reproduction continuously between spawning events by storing energy reserves which are then made available later for spawning, the method even applies if spawning intervals are irregular.

Adaptation. Our method could be particularly useful to study changes in life history parameters over time or differences among populations. Concerns had been raised that life history traits of exploited species, may evolve in response to harvesting (Rijnsdorp 1993, Stokes, et al. 1993, Heino 1998, Law 2000). Studies on life history evolution in the wild have largely focused on changes in the onset of maturation, although evolutionary changes were also suggested in growth rate and reproductive investment (see review in Jørgensen, et al. 2007). The analysis of harvesting-induced evolution in the wild has proved to be difficult (Rijnsdorp 1993, Law 2000, Sinclair, et al. 2002, Conover, et al. 2005). One reason is that growth, maturation and reproductive investment are intricately

linked in the energy allocation schedule, another that disentangling phenotypic plasticity from genetic effects in the observed phenotypic response is not evident

Disentangling plasticity. By estimating the co-variance structure between the life history parameters, our method may prove useful to disentangle phenotypic plasticity from genetic change. Assuming that environmental variability mostly affects the primary energy flow of energy acquisition and that the subsequent energy allocations (maintenance, reproductive investment) are partly determined by this primary energy flow, plastic variation in the other traits due to this process could be accounted for by expressing them conditional on energy acquisition. It is for instance likely that reproductive investment may be affected by feeding conditions during the previous growing season (Rijnsdorp 1990, Stearns 1992, Kjesbu, et al. 1998, Marshall, et al. 1999). Studies in other taxa than fish (e.g. Ernande, et al. 2004) have shown that the energy allocation strategy between maintenance, growth, and reproductive investment may vary according to food availability. Expressing reproductive investment conditional on energy acquisition would therefore represent a reaction norm for reproductive investment (Rijnsdorp, et al. 2005). Changes in this reaction norm would then reveal genetic change under the assumption that most environmental influence on reproductive investment is accounted for via variation in energy acquisition. It has also been shown here that the PMRN can be estimated directly from the back-calculated ages and sizes and the obtained estimate for the age at first maturity, whereas in other data sources the individual first maturity is typically not known (see Barot, et al. 2004). By disentangling the plasticity in maturation caused by variation in growth and removing the effect of survival on observed maturation events, the PMRN can also be used to assess genetic

changes under the assumption that most environmental influence on maturation is accounted for via growth variation.

Different approaches. In an earlier study, Rijnsdorp and Storbeck (1995) estimated the timing of the onset of maturation in plaice by piecewise linear regression of growth increments on body weight to locate the discontinuity in growth rates expected at maturation. This method might be accurate only for particular combinations of the energy allocation scaling exponents that lead to a linear relationship between growth increments and body weight (not shown). Baulier and Heino (2008) applied an improved version of this method to Norwegian spring spawning herring and obtained relatively accurate estimates (± 1 year) of the timing of the onset of maturation. However, this method does not provide estimates of the other life history parameters and it is unlikely that the particular combination of energy allocation scaling exponents leading to the discontinuous linear relationship between growth increments and body weight can be expected to apply in the general case.

The three-trait estimation procedure in the method presented in this paper removes the confounding between parameters by fixing maintenance to its population level average. However, in reality maintenance may be variable since it is affected for instance by temperature and, in addition, assuming a fixed value inflates co-variances between other parameters. A more elegant way to circumvent this problem may be to use generalized linear mixed modeling to estimate the four parameters. Under this approach, the parameters, shown here to be approximately normally distributed after removal of the confounded estimates (Fig.1), follow a multivariate normal distribution and estimation

can thus only lead to unimodal distributions, therefore potentially reducing the confounding between parameters (Brunel, et al. submitted).

The four-trait method presented in this paper is not practical, since the first mode in the distribution of b estimates would always have to be removed *a posteriori*. The three-trait estimation gives more stable results (Figures 4, 5 and 6) but a correction for changing temperatures would be needed (see below) and due to the inflation of co-variances, results should be considered on a relative scale. If the main interest is on the onset of maturation t_{mat}, then both four-trait and three-trait estimation work similarly well, since the bias in t_{mat} is unlikely due to confounding in the parameters a, b and c (Table 4, Figure 4).

Maintenance-Temperature. The estimated energy allocation parameters here represent average values for the study period. However, assuming a constant maintenance (three-trait estimation) may be incorrect as yearly averaged surface temperatures in the North Sea (Van Aken 2008) suggest that temperature increased from 9.91˚C in 1950 to 11.01˚C in 2005 ($p<0.001$). In the interpretation used here, the size-specific maintenance is influenced only by temperature. The Arrhenius description based on the Van't Hoff equation used in dynamic energy budget modeling (Van der Veer, et al. 2001) to describe the effect of temperature on physiological rates would predict that an increase from 10°C to 11°C would correspond to an increase in the maintenance rate of about 9% (not shown). If a similar trend occurred in the bottom temperatures, we might expect a change in the average maintenance cost over the study period of about 9%. In the three-trait estimation, the trend in temperature could therefore be accounted for by estimating a separate average b for each cohort. As this paper explores average general patterns, we

ignored here the effect of temperature on maintenance by assuming homogeneous temperatures in the demersal zone.

Conclusion. This paper is the first one to present a method to estimate the energy allocation parameters for energy acquisition, maintenance, reproductive investment and onset of maturation of organisms from individual growth trajectories. Performance analysis and the application to real data showed that the method can be successfully applied, at least on a qualitative level, to estimate the relative differences in energy allocation parameters between individuals and to estimate their co-variance structure. Future studies will apply the concept to back-calculated growth curves from otoliths of North Sea sole and plaice and scales of Norwegian spring spawning herring, focusing on the comparison between species and life-history adaptation over the last century.

ACKNOWLEDGEMENTS

This research has been supported by the European research training network FishACE funded through Marie Curie (contract MRTN-CT-2204-005578). We thank Ulf Dieckmann and Mikko Heino for conceptual advice, Christian Jørgenson for support in considerations on metabolism, Patrick Burns (**http://www.burns-stat.com/**) for consulting in algorithm programming, Henk Van der Veer for clarifying the dependence of maintenance on temperature in North Sea plaice, and all members of the FishACE and FinE networks for useful discussions.

CITED LITERATURE

Banavar, J. R., Damuth, J., Maritan, A. and Rinaldo, A. 2002. Supply-demand balance and metabolic scaling. - Proceedings of the National Academy of Sciences 99: 10506-10509.

Barot, S., Heino, M., O'Brien, L. and Dieckmann, U. 2004. Estimating reaction norms for age and size at maturation when age at first reproduction is unknown. - Evolutionary Ecology Research 6: 659-678.

Baulier, L. and Heino, M. 2008. Norwegian spring-spawning herring as the test case of piecewise linear regression method for detecting maturation from growth patterns. - Journal of Fish Biology 73: 2452-2467.

Blueweiss, L., Fox, H., Kudzma, V., Nakashima, D., Peters, R. and Sams, S. 1978. Relationships between body size and some life-history parameters. - Oecologia 37: 257-272.

Bolle, L. J., Hunter, E., Rijnsdorp, A. D., Pastoors, M. A., Metcalfe, J. D. and Reynolds, J. D. 2005. Do tagging experiments tell the truth? Using electronic tags to evaluate conventional tagging data. - ICES Journal of Marine Science 62: 236-246.

Brown, J. H., Gillooly, J. F., Allen, A. P., Savage, V. M. and West, G. B. 2004. Toward a metabolic theory of ecology. - Ecology 85: 1771-1789.

Brunel, T., Ernande, B., Mollet, F. M. and Rijnsdorp, A. D. 2009. Estimating age at maturation and energy-based life–history traits from individual growth trajectories with nonlinear mixed-effects models. - Journal of Animal Ecology submitted.

Byrd, R. H., Lu, P., Nocedal, J. and Zhu, C. 1995. A limited memory algorithm for bound constrained optimization. - SIAM J. Scientific Computing 16: 1190–1208.

Charnov, E. L., Turner, T. F. and Winemiller, K. O. 2001. Reproductive constraints and the evolution of life histories with indeterminate growth. - Proceedings of the National Academy of Sciences of the United States of America 98: 9460-9464.

Clarke, A. 2004. Is there a universal temperature dependence of metabolism? - Functional Ecology 18: 252-256.

Colloca, F., Cardinale, M., Marcello, A. and Ardizzone, G. D. 2003. Tracing the life history of red gurnard (*Aspitrigla cuculus*) using validated otolith annual rings. - Journal of Applied Ichthyology 19: 1-9.

Conover, D. O., Arnott, S. A., Walsh, M. R. and Munch, S. B. 2005. Darwinian fishery science: lessons from the Atlantic silverside (*Menidia menidia*). - Canadian Journal of Fisheries and Aquatic Sciences 62: 730-737.

Darveau, C. A., Suarez, R. K., Andrews, R. D. and Hochachka, P. W. 2002. Allometric cascade as a unifying principle of body mass effects on metabolism. - Nature 417: 166-170.

Dawson, A. S. and Grimm, A. S. 1980. Quantitative changes in the protein, lipid and energy content of the carcass, ovaries and liver of adult female plaice, *Pleuronectes platessa* L. - Journal of Fish Biology 16: 493-504.

Day, T. and Taylor, P. D. 1997. Von Bertalanffy's growth equation should not be used to model age and size at maturity. - American Naturalist 149: 381-393.

Ebert, T. A. 1986. A new theory to explain the origin of growth lines in sea urchin spines. - Marine Ecology-Progress Series 34: 197-199.

Engelhard, G. H., Dieckmann, U. and Gødo, O. R. 2003. Age at maturation predicted from routine scale measurements in Norwegian spring-spawning herring (*Clupea harengus*) using discriminant and neural network analyses. - ICES Journal of Marine Science 60: 304-313.

Ernande, B., Boudry, P., Clobert, J. and Haure, J. 2004. Plasticity in resource allocation based life history traits in the Pacific oyster, Crassostrea gigas. I. Spatial variation in food abundance. - Journal of Evolutionary Biology 17: 342-356.

Fonds, M., Cronie, R., Vethaak, A. D. and Van der Puyl, P. 1992. Metabolism, food consumption and growth of plaice (*Pleuronectes platessa*) and flounder (Platichthys flesus) in relation to fish size and temperature. - Netherlands Journal of Sea Research 29: 127-143.

Fraley, C. and Raftery, A. E. 2006. MCLUST Version 3 for R: Normal mixture modeling and model-based clustering. - Department of Statistics, University of Washington Technical Report No. 504.

Francis, R. and Horn, P. L. 1997. Transition zone in otoliths of orange roughy (*Hoplostethus atlanticus*) and its relationship to the onset of maturity. - Marine Biology 129: 681-687.

Gage, J. D. 1992. Natural growth bands and growth variability in the sea urchin *Echinus Esculentus* - results from tetracycline tagging. - Marine Biology 114: 607-616.

Gillooly, J. F., Brown, J. H., West, G. B., Savage, V. M. and Charnov, E. L. 2001. Effects of size and temperature on metabolic rate. - Science 293: 2248-2251.

Godfrey, L. R., Samonds, K. E., Jungers, W. L. and Sutherland, M. R. 2001. Teeth, brains, and primate life histories. - American Journal of Physical Anthropology 114: 192-214.

Grift, R. E., Rijnsdorp, A. D., Barot, S., Heino, M. and Dieckmann, U. 2003. Fisheries-induced trends in reaction norms for maturation in North Sea plaice. - Marine Ecology Progress Series 257: 247-257.

Heino, M. 1998. Management of evolving fish stocks. - Canadian Journal of Fisheries and Aquatic Sciences 55: 1971-1982.

Heino, M. and Kaitala, V. 1999. Evolution of resource allocation between growth and reproduction in animals with indeterminate growth. - Journal of Evolutionary Biology 12: 423-429.

Heino, M., Dieckmann, U. and Godo, O. R. 2002. Measuring probabilistic reaction norms for age and size at maturation. - Evolution 56: 669-678.

Jørgensen, C., Enberg, K., Dunlop, E. S., Arlinghaus, R., Boukal, D. S., Brander, K., Ernande, B., Gardmark, A., Johnston, F., Matsumura, S., Pardoe, H., Raab, K., Silva, A., Vainikka, A., Dieckmann, U., Heino, M. and Rijnsdorp, A. D. 2007. Ecology - Managing evolving fish stocks. - Science 318: 1247-1248.

Kjesbu, O. S., Witthames, P. R., Solemdal, P. and Walker, M. G. 1998. Temporal variations in the fecundity of Arcto-Norwegian cod (*Gadus morhua*) in response to natural changes in food and temperature. - Journal of Sea Research 40: 303-321.

Kooijman, S. A. L. M. 1986. Population dynamics on basis of energy budgets. - In: Metz, J. A. J. and Dieckmann, O. (eds.), The dynamics of physiologically structured populations. Springer-Verlag, pp. 266-297.

Kooijman, S. A. L. M. 2000. Dynamic energy and mass budgets in biological systems. - Cambridge University Press.

Kozlowski, J. 1996. Optimal allocation of resources explains interspecific life history patterns in animals with indeterminate growth. - Proceedings of The Royal Society of London Series B-Biological Sciences 263: 559-566.

Kozlowski, J. and Konarzewski, M. 2004. Is West, Brown and Enquist's model of allometric scaling mathematically correct and biologically relevant? - Functional Ecology 18: 283-289.

Kumbar, S. M. and Pancharatna, K. 2001. Determination of age, longevity and age at reproduction of the frog Microhyla ornata by skeletochronology. - Journal of Biosciences 26: 265-270.

Law, R. 2000. Fishing, selection, and phenotypic evolution. - ICES Journal of Marine Science 57: 659-668.

Laws, R. M. 1952. A new method of age determination for mammals. - Nature 169: 972-973.

Lester, N. P., Shuter, B. J. and Abrams, P. A. 2004. Interpreting the von Bertalanffy model of somatic growth in fishes: the cost of reproduction. - Proceedings of the Royal Society of London Series B Biological Sciences 271: 1625-1631.

Lynch, M. and Walsh, B. 1998. Genetics and analysis of quantitative traits. - Sunderland: Sinauer Associates Inc.

Marshall, C. T., Yaragina, N. A., Lambert, Y. and Kjesbu, O. S. 1999. Total lipid energy as a proxy for total egg production by fish stocks. - Nature 402: 288-290.

Misawa, Y. and Matsui, M. 1999. Age determination by skeletochronology of the Japanese salamander *Hynobius kimurae* (Amphibia, Urodela). - Zoological Science 16: 845-851.

Oskarsson, G. J., Kjesbu, O. S. and Slotte, A. 2002. Predictions of realised fecundity and spawning time in Norwegian spring-spawning herring (*Clupea harengus*). - Journal of Sea Research 48: 59-79.

Panfili, J. and Tomas, J. 2001. Validation of age estimation and back-calculation of fish length based on otolith microstructures in tilapias (Pisces, Cichlidae). - Fishery Bulletin 99: 139-150.

Pearse, J. S. and Pearse, V. B. 1975. Growth zones in echinoid skeleton. - American Zoologist 15: 731-753.

Priede, I. G. and Holliday, F. G. T. 1980. The use of a new tilting tunnel respirometer to investigate some aspects of metabolism and swimming activity of the plaice (*Pleuronectes Platessa* L). - Journal Of Experimental Biology 85: 295-309.

Rijnsdorp, A. D. 1990. The mechanism of energy allocation over reproduction and somatic growth in female North-Sea plaice, *Pleuronectes platessa* L. - Netherlands Journal of Sea Research 25: 279-289.

Rijnsdorp, A. D. 1991. Changes in fecundity of female North-Sea plaice (*Pleuronectes platessa* L) between 3 periods since 1900. - ICES Journal of Marine Science 48: 253-280.

Rijnsdorp, A. D. 1993. Fisheries as a large-scale experiment on life history evolution - disentangling phenotypic and genetic effects in changes in maturation and reproduction of North Sea plaice, *Pleuronectes platessa* L. - Oecologia 96: 391-401.

Rijnsdorp, A. D. and Van Leeuwen, P. I. 1992. Density-dependent and independent changes in somatic growth of female North Sea plaice *Pleuronectes platessa* between 1930 and 1985 as revealed by back-calculation of otoliths. - Marine Ecology-Progress Series 88: 19-32.

Rijnsdorp, A. D. and Pastoors, M. A. 1995. Modeling the spatial dynamics and fisheries of North Sea plaice (*Pleuronectes Platessa* L) based on tagging data. - ICES Journal of Marine Science 52: 963-980.

Rijnsdorp, A. D. and Storbeck, F. 1995. Determining the onset of sexual maturity from otoliths of individual female North Sea plaice, *Pleuronectes platessa* L. - In: Secor, D. H., Dean, J. M. and S., C. (eds.), Recent Developments in Fish Otolith Research. University of South Carolina Press, pp. 581-598.

Rijnsdorp, A. D. and Van Leeuwen, P. I. 1996. Changes in growth of North Sea plaice since 1950 in relation to density, eutrophication, beam trawl effort, and temperature. - ICES Journal of Marine Science 53: 1199-1213.

Rijnsdorp, A. D., Van Leeuwen, P. I. and Visser, T. A. M. 1990. On the validity and precision of back-calculation of growth from otoliths of the plaice, *Pleuronectes platessa* L. - Fisheries Research 9: 97-117.

Rijnsdorp, A. D., Grift, R. E. and Kraak, S. B. M. 2005. Fisheries-induced adaptive change in reproductive investment in North Sea plaice (*Pleuronectes platessa*)? - Canadian Journal of Fisheries and Aquatic Sciences 62: 833-843.

Roff, D. A. 1991. The evolution of life-history variation in fishes, with particular reference to flatfishes. - Netherlands Journal of Sea Research 27: 197-207.

Roff, D. A. 1992. The evolution of life histories. - Chapman & Hall.

Runnström, S. 1936. A study on the life history and migrations of the Norwegian spring-spawning herring based on the analysis of the winter rings and summer zones of the scale. - Fisk Dir. Skr. Ser. Havunders. 5: 1-103.

Savage, V. M., Gillooly, J. F., Woodruff, W. H., West, G. B., Allen, A. P., Enquist, B. J. and Brown, J. H. 2004. The predominance of quarter-power scaling in biology. - Functional Ecology 18: 257-282.

Sinclair, A. F., Swain, D. P. and Hanson, J. M. 2002. Measuring changes in the direction and magnitude of size-selective mortality in a commercial fish population. - Canadian Journal of Fisheries and Aquatic Sciences 59: 361-371.

Smith, S. L. 2004. Skeletal age, dental age, and the maturation of KNM-WT 15000. - American Journal of Physical Anthropology 125: 105-120.

Snover, M. L. and Hohn, A. A. 2004. Validation and interpretation of annual skeletal marks in loggerhead (*Caretta caretta*) and Kemp's ridley (*Lepidochelys kempii*) sea turtles. - Fishery Bulletin 102: 682-692.

Stearns, S. C. 1992. The evolution of life histories. - Oxford University Press.

Stevenson, R. D. and Woods Jr., W. A. 2006. Condition indices for conservation: New uses for evolving tools. - Integrative and Comparative Biology 46: 1169-1190.

Stokes, T. K., McGlade, J. M. and Law, R. 1993. The exploitation of evolving resources. - Springer-Verlag.

Van Aken, H. M. 2008. Variability of the water temperature in the western Wadden Sea on tidal to centennial time scales. - Journal of Sea Research 60: 227-234.

Van der Veer, H. W., Kooijman, S. A. L. M. and Van der Meer, J. 2001. Intra- and interspecies comparison of energy flow in North Atlantic flatfish species by means of dynamic energy budgets. - Journal of Sea Research 45: 303-320.

Videler, J. J. and Nolet, B. A. 1990. Costs of swimming measured at optimum speed - scale effects, differences between swimming styles, taxonomic groups and submerged and surface swimming. - Comparative Biochemistry and Physiology a-Physiology 97: 91-99.

Von Bertalanffy, L. and Pirozynski, W. J. 1952. Tissue respiration, growth, and basal metabolism. - Biological Bulletin 105: 240-256.

Ware, D. M. 1982. Power and evolutionary fitness of teleosts. - Canadian Journal of Fisheries and Aquatic Sciences 39: 3-13.

West, G. B., Brown, J. H. and Enquist, B. J. 1997. A general model for the origin of allometric scaling laws in biology. - Science 276: 122-126.

West, G. B., Brown, J. H. and Enquist, B. J. 1999. The fourth dimension of life: Fractal geometry and allometric scaling of organisms. - Science 284: 1677-1679.

West, G. B., Brown, J. H. and Enquist, B. J. 2001. A general model for ontogenetic growth. - Nature 413: 628-631.

Witbaard, R., Franken, R. and Visser, B. 1997. Growth of juvenile Arctica islandica under experimental conditions. - Helgolander Meeresuntersuchungen 51: 417-431.

Witbaard, R., Duineveld, G. C. A. and de Wilde, P. 1999. Geographical differences in growth rates of *Arctica islandica* (Mollusca : Bivalvia) from the North Sea and adjacent waters. - Journal of the Marine Biological Association of the United Kingdom 79: 907-915.

Zug, G. R., Balazs, G. H., Wetherall, J. A., Parker, D. M. and Murakawa, S. K. K. 2002. Age and growth of Hawaiian green seaturtles (*Chelonia mydas*): an analysis based on skeletochronology. - Fishery Bulletin 100: 117-127.

APPENDIX

Switch. To switch from juvenile to adult growth at t_{mat} in (1), a logistic function is used:

$$S(t) = \frac{1}{1 + e^{-k(t - t_{\mathrm{mat}})}} \qquad \text{[A1]}$$

where k is any number large enough so that S(t) switches almost immediately from 0 to 1 as soon as $t > t_{mat}$, thus approximating a Heaviside step function.

Reproductive investment. The reproductive investment $R(t + \Delta t)$ is given by the rate of energy conversion to reproduction $cw(t)$ integrated over the period from t to $t + \Delta t$, expressed as a function of the somatic weights at the start $w(t)$ and at the end $w(t + \Delta t)$ of the time interval Δt, over which the reproductive events repeatedly occur. Assuming $\alpha = 3/4$ and $\beta = \gamma = 1$,

$$R(t + \Delta t) = \int_{t}^{t+\Delta t} cw(\tau)d\tau = \int_{w(t)}^{w(t+\Delta t)} \frac{c}{aw^{\alpha} - (b+c)w} dw = \ldots$$

$$= \frac{c}{b+c}\Bigg[w_t - w_{t+\Delta t} + \frac{4a}{3(b+c)}(w_t^{3/4} - w_{t+\Delta t}^{3/4}) + \frac{2a^2}{(b+c)^2}(w_t^{1/2} - w_{t+\Delta t}^{1/2})$$

$$+ \frac{4a^3}{(b+c)^3}(w_t^{1/4} - w_{t+\Delta t}^{1/4}) + \frac{4a^4}{(b+c)^4}\left(\log(a - (b+c)w_t^{1/4}) - \log(a - (b+c)w_{t+\Delta t}^{1/4})\right)\Bigg] \qquad \text{[A2]}$$

Code. A code example follows to illustrate the applied estimation method for one single fish (object grodat). The weight scaling exponent α of energy acquisition rate, weight at

age 0 w_0, the expected population averages (used to define the staring values), the boundaries for age at maturation t_{mat} and the asymptotic weight w_∞ are species-specific. The function indest runs the optimization (optimfun) over a grid of staring values, removes aberrant estimates, returns the best fit and plots the fitted curve.

```
#define weight scaling, weight at age 0 and the switch parameter
alpha<-3/4
w0<-0.0025
swi<-1e12

#individual growth data with at least 4 observations, age and weight in columns
grodat<-data.frame(age=0:10,
                   weight=c(w0,4.0,33.5,143.5,301.7,443.3,546.3,614.3,706.8,766.5,829.5))

#define biological parameter boundaries boundaries
lo.a<-1e-10;up.a<-Inf
lo.b<-1e-10;up.b<-Inf
lo.c<-1e-10;up.c<-Inf
lo.tmat<-2/3;up.tmat<-26/3
lo.Winf<-400;up.Winf<-4000

limit<-
matrix(c(lo.a,lo.b,lo.c,lo.tmat,lo.Winf,up.a,up.b,up.c,up.tmat,up.Winf),nrow=2,byrow=T,
            dimnames=list(c("lower","upper"),c("a","b","c","tmat","Winf")))

#estimated or expected population averages
a_pop<-4.84
b_pop<-0.475
c_pop<-0.398
tmat_pop<-4.00

#growth function
grofun<-function(a,b,c,t,tmat,alpha)
{
  j = 1-alpha
  S = 1/(1+exp(-swi*(t-tmat)))
  wmat = (a/b - (a/b - w0^j)*exp(-b*tmat*j))^(1/j)
  W = ((1 - S)*(a/b - (a/b - w0^j)*exp(-t*b*j)) + S*(a/(b+c)-(a/(b+c) - wmat^j)*exp(-
(b+c)*(t-tmat)*j)))^(1/j)
  return(W)
}

#fitting function
indest<-function(grodat,limit,stlen,alpha)
{
  PARS<-
as.data.frame(matrix(NA,nrow=1,ncol=7,dimnames=list(1,c("a","b","c","tmat","Winf","wmat",
"goodness"))))
  j = 1 - alpha

  tmat.uplim<-min(c(max(grodat$age)-1/3,limit[2,4]))

  optimfun<-function(pars)
  {
    a<-pars[1];b<-pars[2];c<-pars[3];tmat<-pars[4]
    tage<-grodat$age
    S = 1/(1+exp(-swi*(tage-tmat)))
    wmat = (a/b - (a/b - w0^j)*exp(-b*tmat*j))^(1/j)
    W = ((1 - S)*(a/b - (a/b - w0^j)*exp(-tage*b*j)) + S*(a/(b+c) -(a/(b+c) -
wmat^j)*exp(-(b+c)*(tage-tmat)*j)))^(1/j)
    ssr<-sum((grodat$weight-W)^2)
    return(ssr)
```

```
  }

  st.a<-seq((a_pop-0.25*a_pop),(a_pop+0.25*a_pop),len=stlen)
  st.b<-seq((b_pop-0.25*b_pop),(b_pop+0.25*b_pop),len=stlen)
  st.c<-seq((c_pop-0.25*c_pop),(c_pop+0.25*c_pop),len=stlen)
  st.tmat<-seq((tmat_pop-
0.5*tmat_pop),min(c(tmat.uplim,(tmat_pop+0.5*tmat_pop))),len=stlen)

  stval<-
expand.grid(st.a=st.a,st.b=st.b,st.c=st.c,st.tmat=st.tmat,a=NA,b=NA,c=NA,tmat=NA,RSE=NA)
  stval$st.Winf<-(stval$st.a/(stval$st.b+stval$st.c))^(1/j)
  stval<-stval[(stval$st.Winf>=limit[1,5])&(stval$st.Winf<=limit[2,5]),]

  for(x in 1:nrow(stval))
  {
    pars<-c(stval$st.a[x],stval$st.b[x],stval$st.c[x],stval$st.tmat[x])
    if(class(try(Eamod<-optim(par=pars,fn=optimfun,method="L-BFGS-B",lower=c(limit[1,-
5]),upper=c(limit[2,c(1:3)],tmat.uplim)),silent=TRUE))!="try-error")
    {
      stval$a[x]<-Eamod$par[1]
      stval$b[x]<-Eamod$par[2]
      stval$c[x]<-Eamod$par[3]
      stval$tmat[x]<-Eamod$par[4]
      stval$RSE[x]<-Eamod$value
    }
  }

  stval$Winf<-(stval$a/(stval$b+stval$c))^(1/j)
  stval$wmat<-(stval$a/stval$b - (stval$a/stval$b - w0^j)*exp(-
stval$b*stval$tmat*j))^(1/j)
  v.use<-
na.omit(stval[(stval$Winf>=stval$wmat)&(stval$Winf>limit[1,5])&(stval$Winf<limit[2,5])&(s
tval$a>limit[1,1])&(stval$b>limit[1,2])&(stval$c>limit[1,3]),])

  if(nrow(v.use)>0)
  {
    maxfit<-v.use[v.use$RSE==min(v.use$RSE,na.rm=T),]
    PARS$a<-unique(maxfit$a)
    PARS$b<-unique(maxfit$b)
    PARS$c<-unique(maxfit$c)
    PARS$tmat<-unique(maxfit$tmat)
    PARS$wmat<-unique(maxfit$wmat)
    PARS$goodness<-unique(maxfit$RSE)
    PARS$Winf<-unique(maxfit$Winf)
  }

plot(grodat$age,grodat$weight,xlim=c(0,max(grodat$age)+2),ylim=c(0,max(grodat$weight)+100
),xlab="age",ylab="weight")
  if(nrow(na.omit(PARS))>0)
  {

lines(seq(0,30,by=0.1),grofun(a=PARS$a,b=PARS$b,c=PARS$c,t=seq(0,30,by=0.1),tmat=PARS$tma
t,alpha=alpha),col=4)
   abline(v=PARS$tmat,lty=3,col=3)
  }
  return(PARS)
}

indest(grodat=grodat,limit=limit,stlen=5,alpha=alpha)
```

Table 1: Average of percentage bias $\mu\%$, coefficient of variation CV and correlations $r_e(x,x')$ between biases $e(x)$ and $e(x')$ in the estimates of the life history parameters a, b, c and t_{mat} resulting from the four-trait estimation procedure applied to simulated data with (stochastic) and without (deterministic) environmental noise.

	Deterministic				
	$e(a)$	$e(b)$	$e(c)$	$e(b+c)$	$e(t_{\text{mat}})$
$\mu\%$	0.00	0.01	-0.02	0.00	0.00
CV	11.91	8.91	5.52	16.84	21.33
$r_e(a,x')$	1				
$r_e(b,x')$	0.47	1			
$r_e(c,x')$	-0.19	-0.40	1		
$r_e(b+c,x')$	0.36	0.18	0.53	1	
$r_e(t_{mat},x')$	-0.09	0.60	-0.07	0.17	1
	Stochastic				
	$e(a)$	$e(b)$	$e(c)$	$e(b+c)$	$e(t_{\text{mat}})$
$\mu\%$	-0.15	-0.32	0.23	-0.18	0.30
CV	1.34	2.03	3.85	1.45	2.57
$r_e(a,x')$	1				
$r_e(b,x')$	0.83	1			
$r_e(c,x')$	-0.38	-0.67	1		
$r_e(b+c,x')$	0.94	0.76	-0.21	1	
$r_e(t_{mat},x')$	-0.07	0.17	-0.27	0.00	1

Table 2: Results of the regression analysis of the overall bias in life history parameters (Eq. 5) as a function of the potentially explanatory variables (Eq. 8) from a backward selection. Explanatory variables tested comprised of the coefficients of variation CV_a, CV_b, CV_c, the degree of autocorrelation θ_a, θ_b, θ_c, and the correlations $r_{\text{sim}}(a,b)$, $r_{\text{sim}}(a,c)$, $r_{\text{sim}}(b,c)$ of the simulated time series a_t, b_t, c_t, the age t (i.e. the number of simulated data points) the number of experienced spawning events y_{mat}, the relative reproductive investment q, relative timing of onset of maturation τ, and relative initial weight ν_0.

	four-trait estimation		**three-trait estimation**	
Selected variables	**coefficient**	**p-value**	**coefficient**	**p-value**
Intercept β_0	1.031	$< 10^{-3}$	0.475	$< 10^{-3}$
CV_a	0.418	$< 10^{-3}$	2.092	$< 10^{-3}$
CV_c	-	-	-0.245	$< 10^{-3}$
θ_a	-	-	0.032	0.087
θ_c	-	-	-0.026	0.066
$r_{\text{sim}}(a,b)$	-0.066	0.002	-	-
$r_{\text{sim}}(a,c)$	-	-	-0.085	0.001
age t	-0.033	$< 10^{-3}$	0.014	$< 10^{-3}$
y_{mat}	0.044	$< 10^{-3}$	-	-
q	-0.754	$< 10^{-3}$	-	-
τ	0.047	$< 10^{-3}$	-0.119	$< 10^{-3}$
ν_0	-	-	-30540	0.017

Table 3: Energy allocation parameters estimated for the1779 individual North Sea plaice growth trajectories using the four-trait and the three-trait model. The table gives the average μ and coefficient of variation CV, as well as the correlation coefficient $r(x, x')$ between the four life history parameters: energy acquisition a, maintenance b, reproductive investment c and onset of maturation t_{mat}. For the four-trait estimation the results are displayed for only those estimations that belong to the second mode in the distribution of b's.

	four-trait estimation: 2nd b-mode				
	a	b	c	$(b+c)$	t_{mat}
μ	5.31	0.57	0.32	0.90	4.45
CV	0.23	0.62	0.74	0.28	0.37
$r(a, x')$	1				
$r(b, x')$	0.69	1			
$r(c, x')$	-0.06	-0.71	1		
$r(b+c, x')$	0.93	0.74	-0.06	1	
$r(t_{mat}, x')$	-0.22	0.30	-0.63	-0.18	1
	three-trait estimation: fixed b				
	a	b	c	$(b+c)$	t_{mat}
μ	5.29	0.47	0.41	0.89	3.53
CV	0.20	-	0.52	0.24	0.49
$r(a, x')$	1				
$r(b, x')$	-	-			
$r(c, x')$	0.91	-	1		
$r(b+c, x')$	0.91	-	1	1	
$r(t_{mat}, x')$	-0.68	-	-0.64	-0.64	1

Table 4: Estimated against true age at first maturity A_{mat} in the 4- and three-trait estimation. The number of estimations falling in a true A_{mat} class is given as a percentage of the total number of estimations in that true A_{mat} class. The upper panel presents performances for age at maturation estimation by showing true against estimated A_{mat} in the four-trait (simulated data set in which a, b and c vary stochastically), and the three-trait estimation (simulated data set in which a and c vary stochastically). Performance is slightly better for the three-trait estimation. Notice that the biases might not be representative for the real situation, since the simulated CV's might be higher than those applying in nature. The lower panel presents results of the application to real data by comparing the estimation of A_{mat} between the four-trait and the three-trait estimation for both the entire data set and only the observations belonging to the 2nd b-mode. Agreement between the t_{mat} estimates in the four- and three-trait estimation is very high and does not significantly change between the entire data set and the selected observations belonging to the 2nd b-mode. This indicates that the estimation of t_{mat} or A_{mat} is not affected by confounding.

1) Performance analysis

four-trait simulated		True A_{mat}					
		2	3	4	5	6	7
Estimated A_{mat}	2	4	3	2	1	1	0
	3	15	16	8	7	2	1
	4	17	19	31	19	7	1
	5	17	19	21	32	22	5
	6	19	15	12	16	37	14
	7	13	12	11	11	15	22

three-trait simulated		True A_{mat}					
		2	3	4	5	6	7
Estimated A_{mat}	2	30	28	15	10	8	5
	3	18	23	3	1	1	0
	4	21	29	55	9	2	1
	5	15	10	17	59	19	4
	6	8	4	4	13	54	15
	7	5	2	3	4	14	59

2) Application to real data

2nd b-mode observations		three-trait A_{mat}					
		2	3	4	5	6	7
four-trait A_{mat}	2	30	6	0	0	0	0
	3	21	68	7	0	0	1
	4	8	13	63	8	0	0
	5	0	1	22	64	13	1
	6	24	3	4	23	67	12
	7	8	1	1	3	17	71

All real data observations		three-trait A_{mat}					
		2	3	4	5	6	7
four-trait A_{mat}	2	39	8	0	0	0	0
	3	19	76	13	0	0	1
	4	7	8	67	12	0	0
	5	0	0	15	65	16	2
	6	21	2	3	19	65	14
	7	7	0	1	3	16	69

Figure 1: Density distributions of the four estimated parameters on real data. The first mode in the density distribution of maintenance b (solid line) is likely an artifact due to confounding and corresponds to the second mode in the distribution of reproductive investment c. By selecting only observations belonging to the second mode fitted by a Gaussian mixture over parameter b, the first mode in the distribution of b's and the bump to the right in the distribution of c's are removed (dotted thick line).

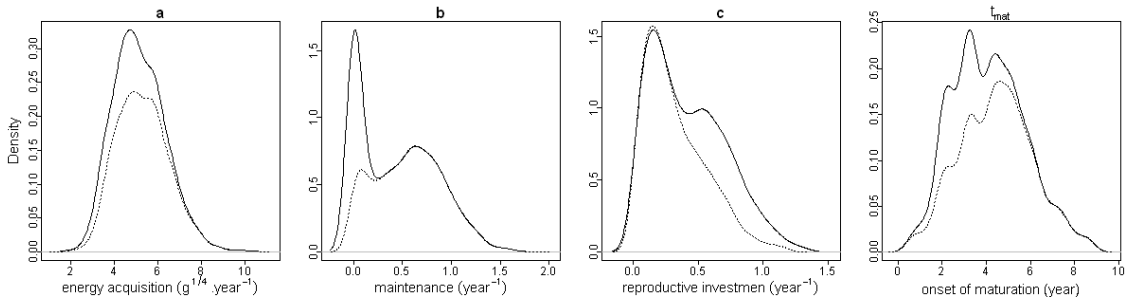

Figure 2: Population fit of life-history on somatic size at age (solid lines) and estimated reproductive investment (dashed lines, see text). Error bars show 5% and 95% confidence intervals for the observations. For the gonads the averages of only mature fish are given whereas the fitted curve represents average population gonadic growth. The estimated life history parameters are a = 4.84 $g^{1/4}yr^{-1}$, b = 0.47 yr^{-1}, c = 0.40 yr^{-1}, t_{mat} = 4.00 yr.

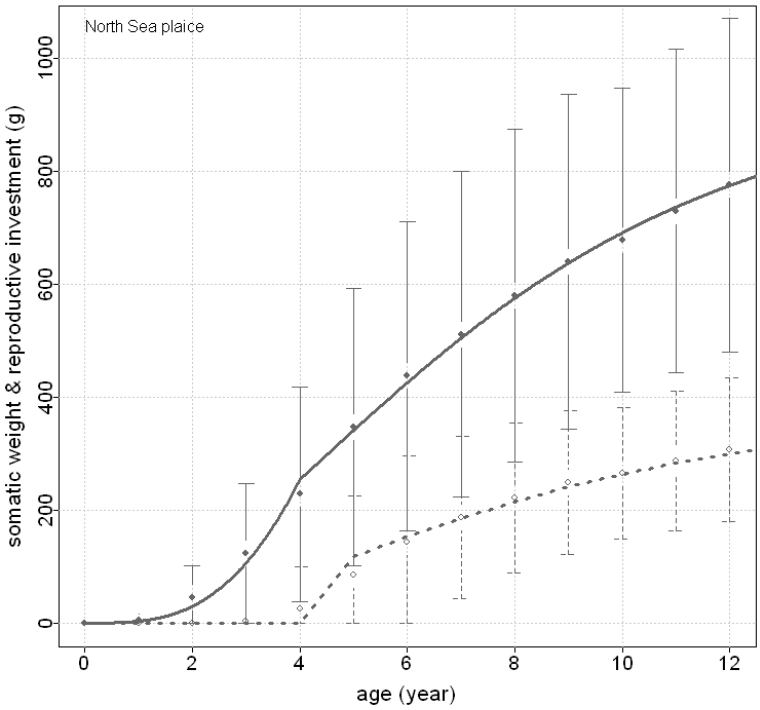

Figure 3: Relationships of reproductive investment relative to size (RSI) and gonadic and migratory investment relative to total reproductive investment (GRI and MRI) as a function of size in the estimation of size-dependent reproductive investment. Because the probability of being mature depends also on age, the RSI slightly changes with age (see gray scale, the darker the older). The GRI has minimal contribution of 86% at a length of about 30cm and increases thereafter. The cost of migration or MRI is accordingly maximal (14%) at this size.

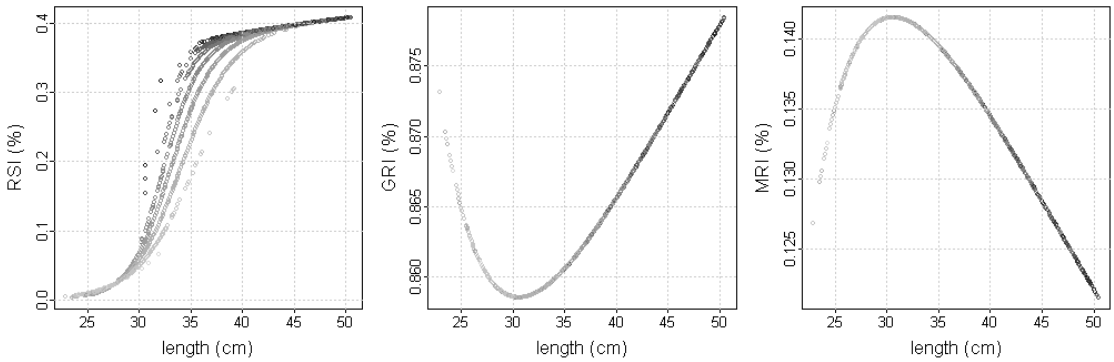

Figure 4: Overall relative bias (Eq. 5) as a function of the true relative reproductive investment q, the true relative onset of maturation τ, the true relative initial size ν_0 and the number of years after the first spawning event y_{mat} (rounded up ($A_{\mathrm{mat}} - t_{\mathrm{mat}}$)) in the deterministic case of the four-trait and the three-trait estimation. The simulation was based on all possible combinations for the observed ranges of the parameters: a {4,7} $\mathrm{g}^{1/4}\mathrm{yr}^{-1}$, b {0.4,0.9} yr^{-1}, c {0.05,0.55} yr^{-1} and t_{mat} {1.25,5.25} yr. Contours were obtained by fitting a non-parametric loess regression to the bias with span = 0.25 for the two explanatory variables to be displayed. Bias becomes considerable if there are few observations y_{mat} of the mature status, if the relative onset of maturation τ is very early and if the relative reproductive investment q is small. Similar trends are found in the three-trait estimation but with lower relative biases and q seems to have no more influence on the bias.

Four-trait estimation

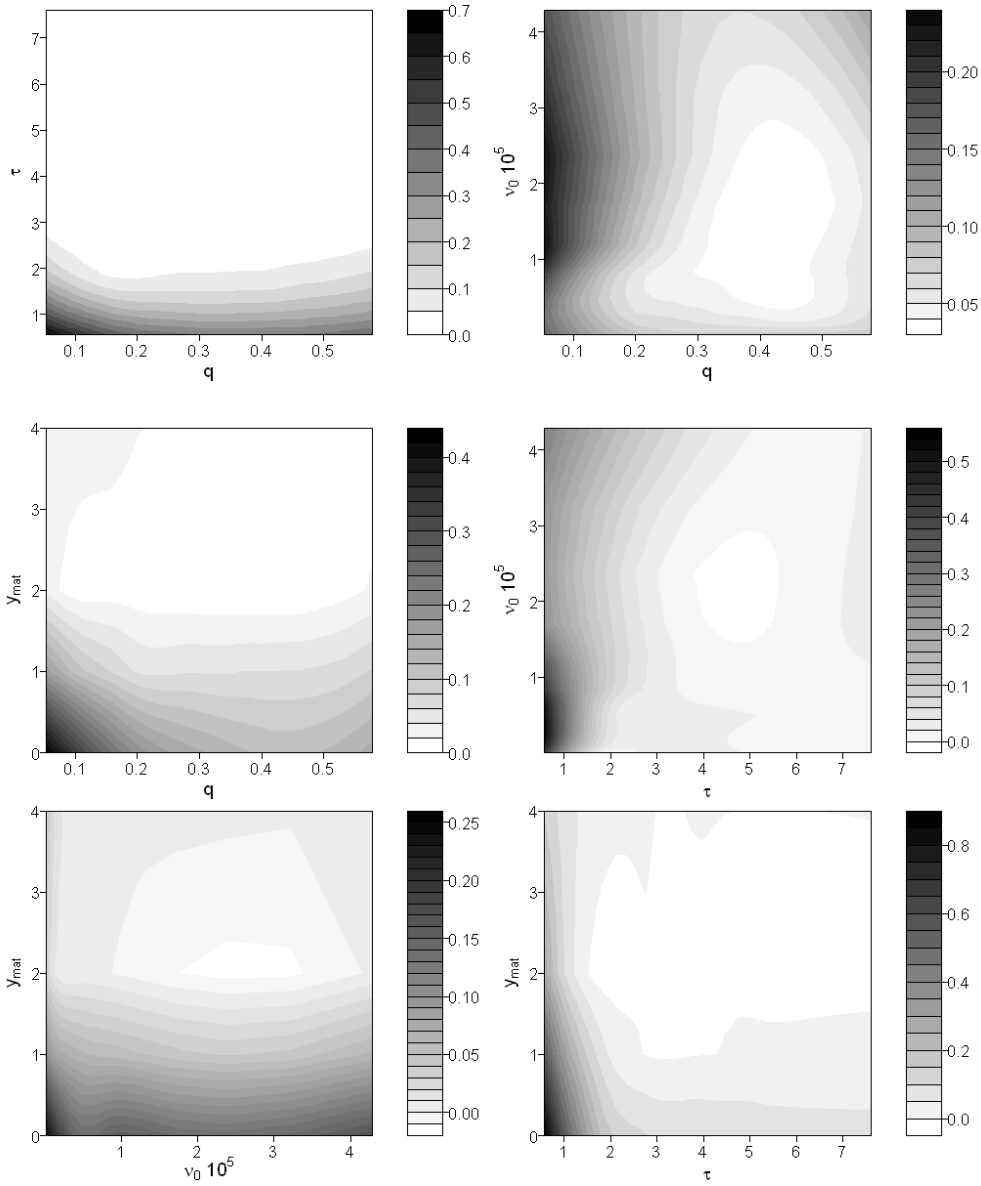

Three-trait estimation

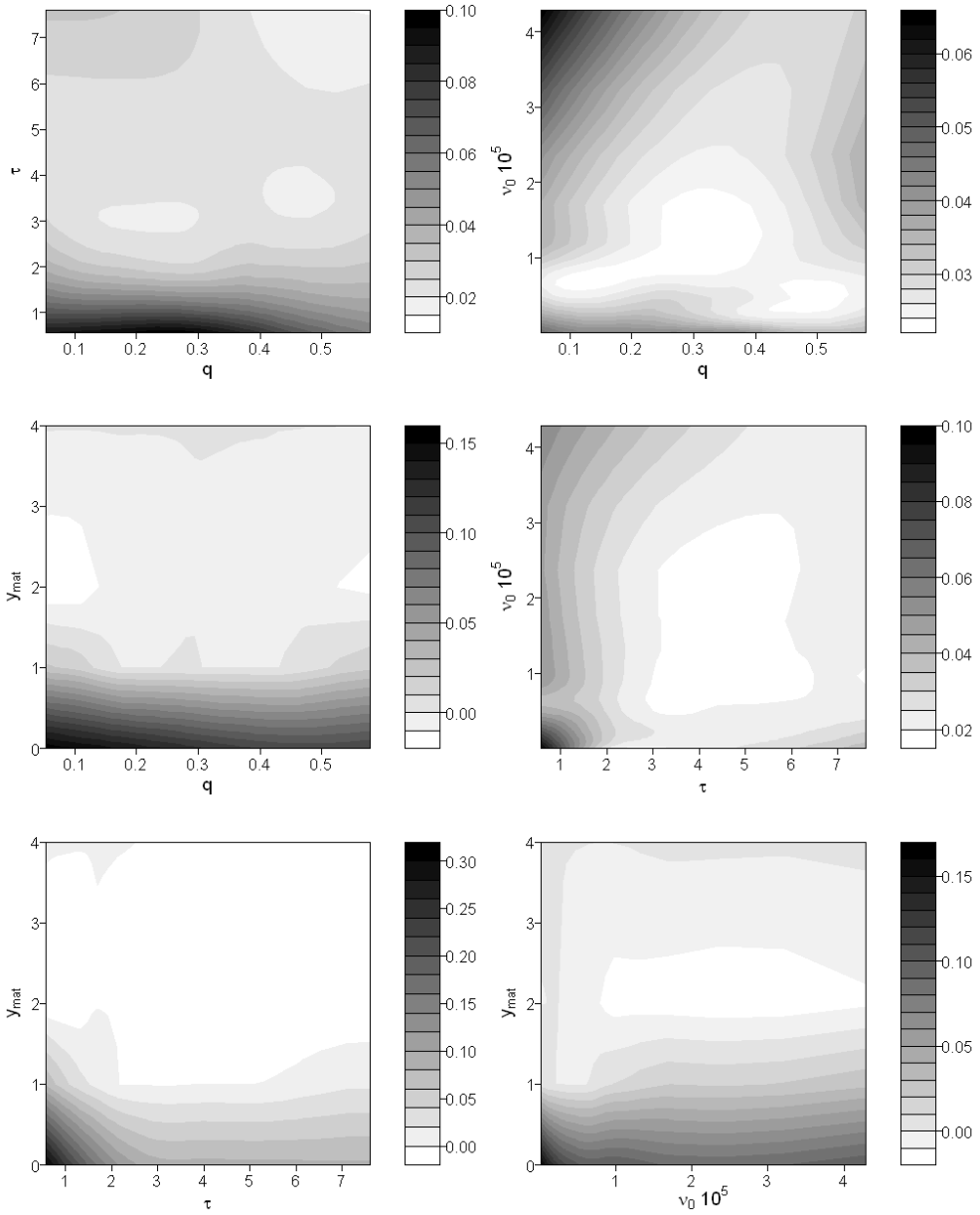

Figure 5: Density distributions of the four estimated life history parameters and relationships between parameter biases estimated on simulated data with environmental noise. Very similar parameter distributions as from real data (see Figure 1) are obtained in the simulation (first row), in which the covariance structure from the selected distribution modes from real data was used. The regressions between parameter biases (dashed lines) show that the biases of b and c are negatively correlated, whereas the bias of $(b+c)$ is on average smaller than bias of each of its components. The strong positive correlation between a and $(b+c)$ is a consequence of fitting to an asymptotic size: the higher a is, the higher $(b+c)$ has to be to reach the same asymptotic size. The same effect translates to b but not to c.

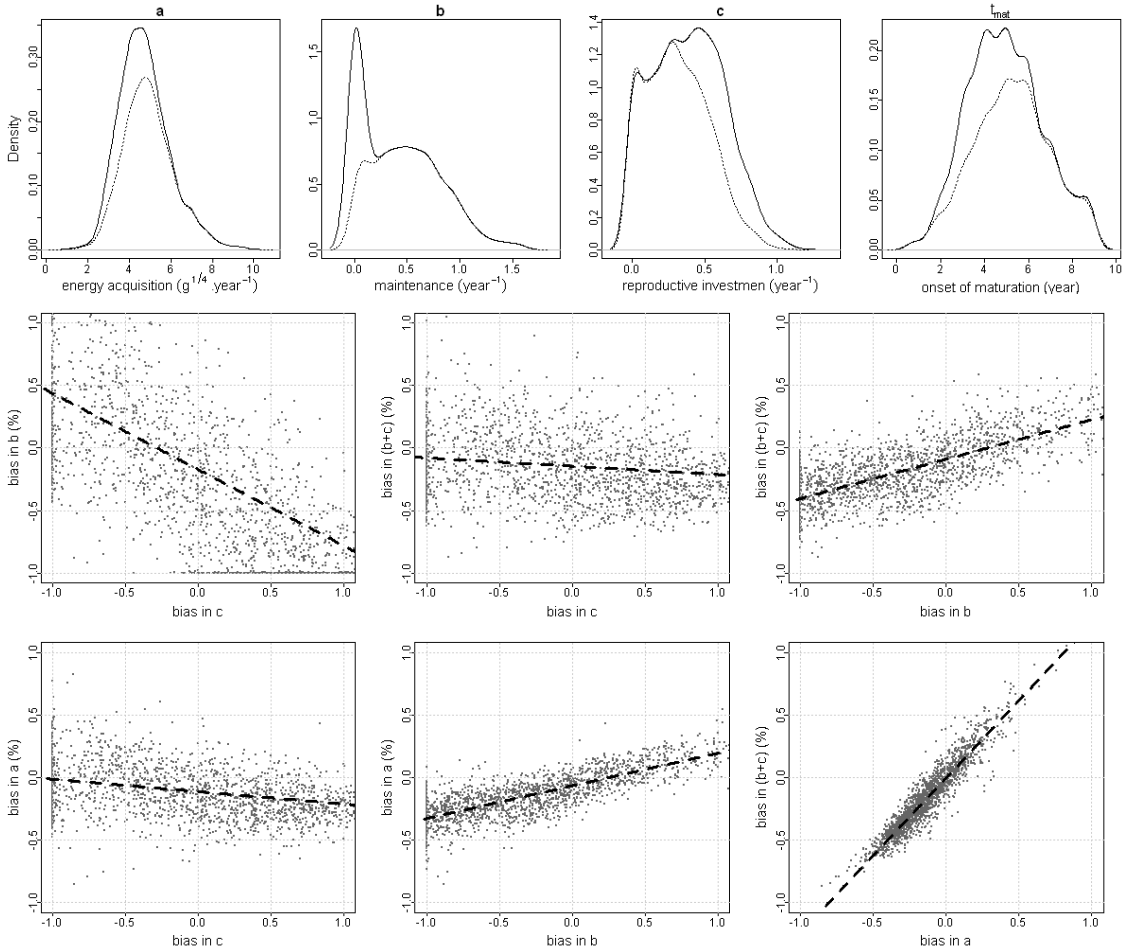
a
b
c
t_{mat}
Density
energy acquisition ($g^{1/4}$ $year^{-1}$)
maintenance ($year^{-1}$)
reproductive investmen ($year^{-1}$)
onset of maturation (year)
bias in b (%)
bias in (b+c) (%)
bias in (b+c) (%)
bias in a (%)
bias in a (%)
bias in (b+c) (%)
bias in c
bias in c
bias in b
bias in c
bias in b
bias in a

Figure 6: Relative biases in a, b, c and t_{mat} in the four-trait estimation and a, c and t_{mat} in the three-trait estimation, resulting from environmental variation, shown as a function of the CV in the simulated time series of a, b, and c (four-trait estimation) or a and c (three-trait estimation). The estimated parameters are given relative to the geometric mean of the time series of a, b, and c. The CV is given by the geometric mean of the realized CV's in series of a, b and c. Black lines show a quantile regression through these biases for the 50% (dashed line) and the 5% and 95% quantiles (dotted lines). Notice that the biases are strictly evaluated only for t_{mat}, since the true reference values of the varying a, b and c is not really known. Furthermore the simulated CV's might be higher than those applying in nature.

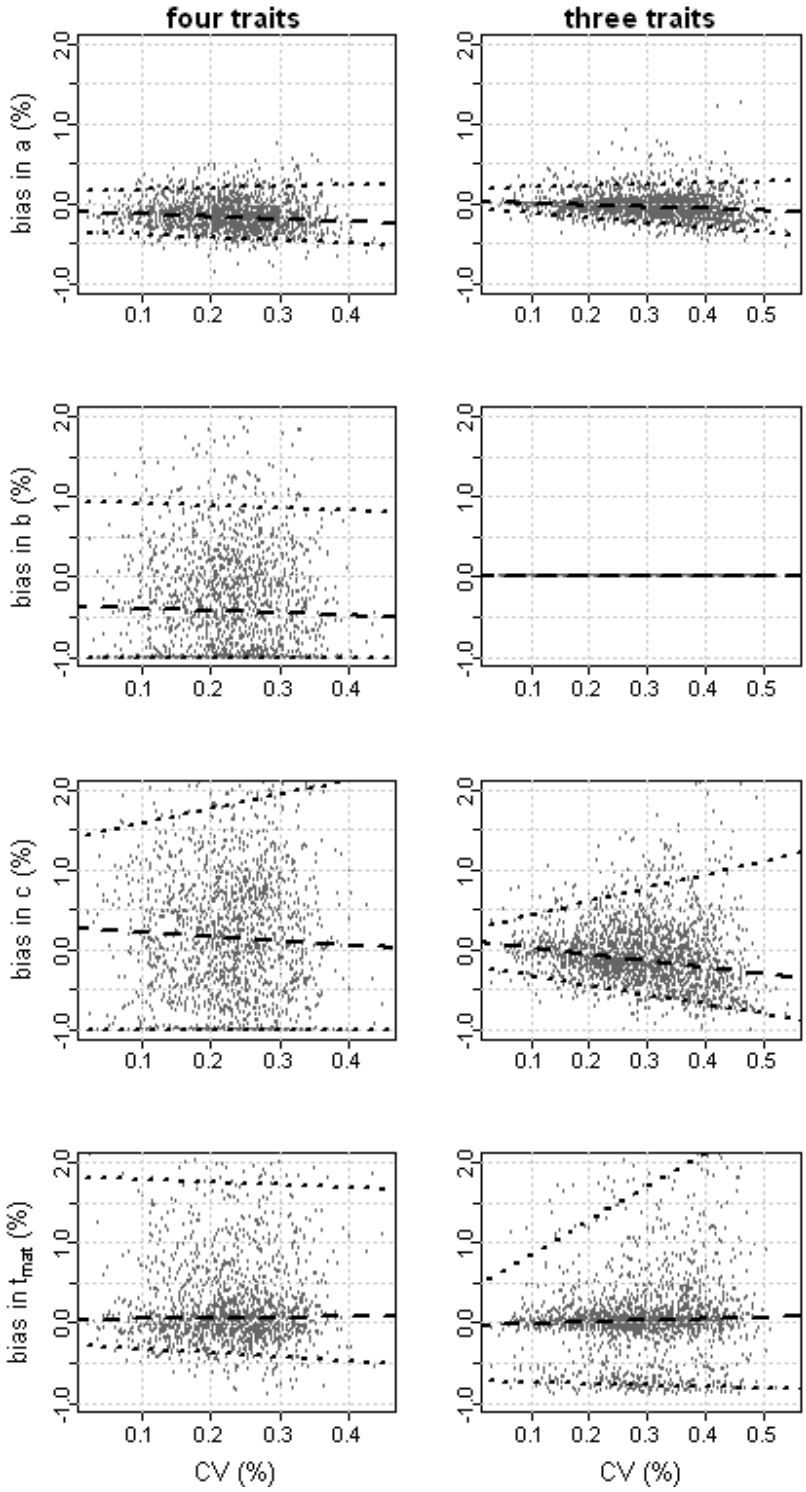
four traits
three traits
bias in a (%)
bias in b (%)
bias in c (%)
bias in t_{mat} (%)
CV (%)
CV (%)

1170

Figure 7: Sensitivity of the parameters estimates a, b, c and t_{mat} to an incorrect assumption about the allometric scaling exponent α ($\alpha_{\mathrm{sim}} = 3/4$ whereas $\alpha_{\mathrm{fit}} = 2/3$ or $\alpha_{\mathrm{fit}} = 4/5$) in the four- and the three-trait estimation. It was accounted for that different allometric scaling exponents would result in different assumptions about the constant maintenance by fitting the energy allocation model to the population growth curve ($b_{\alpha=2/3}$=0.175 year^{-1}, $b_{\alpha=3/4}$=0..459 year^{-1}, $b_{\alpha=4/5}$=0.864 year^{-1}, leading to different solutions of Eq. 4). The estimated against the true parameters are shown, black dots representing the estimates assuming the correct allometric scaling exponent ($\alpha = 3/4$), typically on the 45°-line, light gray "-" and dark gray "+" represent the estimates by assuming falsely a too low ($\alpha = 2/3$) or too high ($\alpha = 4/5$) scaling exponent respectively, whereas the light grey and dark gray dotted lines represent the regression through these estimated and true data points assuming wrong scaling.

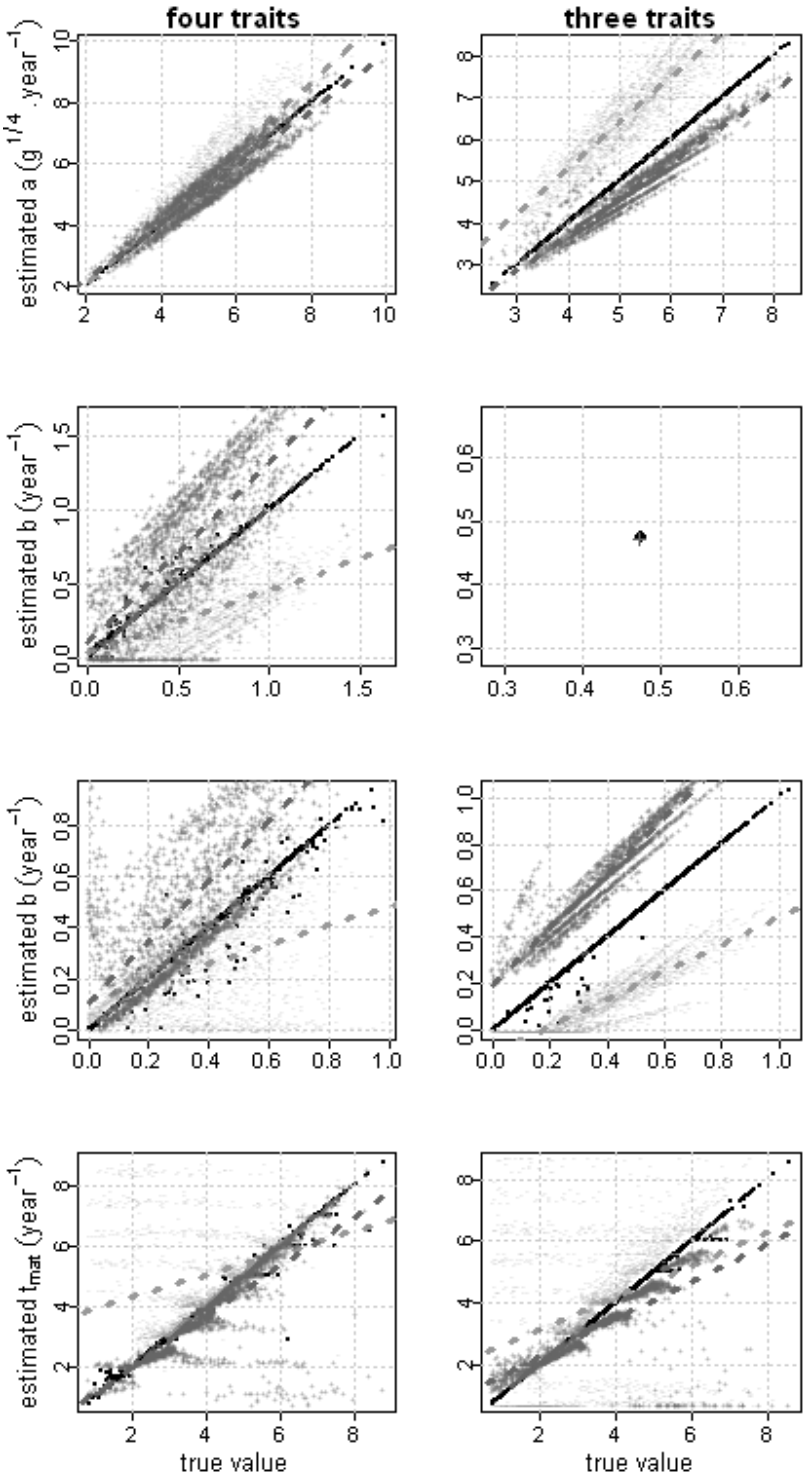
four traits
three traits
estimated a (g^1/4 .year^-1)
estimated b (year^-1)
estimated b (year^-1)
estimated t_mat (year^-1)
true value
true value

1184

Figure 8: Comparison of reaction norms derived from the 3 trait estimation of individual life history in this study (gray lines) with reaction norm estimated by from Grift, et al. (2003) averaged over the past 5 decades by only using cohorts for which more than 30 observations were available. Dotted lines represent the 25%- and 75% probabilities of maturation, the dashed line represents the average length at age. The reaction norm from individual life history estimation is shown for an interpretation of the first spawning event A_{mat} given by t_{mat} plus a minimal period of preparation for spawning of 4 months, rounded up to the next year.